Structure and sedimentology of George VI Ice Shelf, Antarctic Peninsula: implications for ice-sheet dynamics and landform development

MICHAEL J. HAMBREY[1*], BETHAN J. DAVIES[1,2], NEIL F. GLASSER[1], TOM O. HOLT[1], JOHN L. SMELLIE[3] & JONATHAN L. CARRIVICK[4]

[1]*Centre for Glaciology, Department of Geography and Earth Sciences, Aberystwyth University, Aberystwyth, Ceredigion, SY23 3DB, UK*

[2]*Centre for Quaternary Research, Department of Geography, Royal Holloway, University of London, Egham, Surrey, TW20 0EX, UK*

[3]*Department of Geology, University of Leicester, Leicester LE1 7RH, UK*

[4]*School of Geography and water@leeds, University of Leeds, Leeds LS2 9JT, UK*

**Corresponding author (e-mail: mjh@aber.ac.uk)*

Abstract: Collapse of Antarctic ice shelves in response to a warming climate is well documented, but its legacy in terms of depositional landforms is little known. This paper uses remote-sensing, structural glaciological and sedimentological data to evaluate the evolution of the ~25,000 km^2 George VI Ice Shelf, SW Antarctic Peninsula. The ice shelf occupies a north-south-trending tectonic rift between Alexander Island and Palmer Land, and is nourished mainly by ice streams from the latter region. The structure of the ice shelf is dominated by inherited foliation and fractures, and with velocity data indicates a largely compressive flow regime. The formation of a moraine complex at the margin of the ice shelf is controlled by debris entrained within foliation and folds. This englacial debris is of basal origin, and includes both local Mesozoic sedimentary and volcanic lithologies, and exotic crystalline rocks from Palmer Land. Folding of basal ice to a high level in the source glaciers on Palmer Land is required to bring the debris to the surface. These results have implications for understanding flow dynamics of ice shelves under compressive flow, and debris entrainment and moraine formation associated with palaeo-ice shelves.

[191 words]

Supplementary material: *photographs of ice-shelf morphology, ice facies and ice structure; detailed descriptions of ice facies, including foliation logs, supporting*

evidence for interpreting sedimentary facies; complete data-set of sedimentological data, including triangular plots of clast shape, clast roundness histograms, particle-size distribution of sand-size and lower, and pie chart of local clasts versus exotic clasts from Palmer Land; and a table summarising the characteristics of representative clasts in the ice-shelf moraine, based on thin-section analysis, with indication of their provenance.

Interpreting the dynamics and history of ice shelves is important for evaluating the response of ice sheets to climatic and oceanographic changes. Ice shelves have received considerable attention in the Antarctic Peninsula, as they have undergone sequential, rapid collapse (Vaughan & Doake 1996; Morris & Vaughan 2003; Cooke *et al.* 2005; Cook & Vaughan 2010), following a long period during which their grounding-lines had been stable (Rebesco *et al.* 2014). A detailed understanding of ice-shelf character and behaviour is therefore of immediate interest, yet the geological record of ice shelves is largely unknown. Geological and structural glaciological data can provide vital information concerning the evolution of ice shelves over time. However, apart from a few examples of moraines produced by floating glacier ice in the Canadian Arctic Archipelago (England et al. 1978, 2009; England 1999; Hodgson 1984, 1994) and northern Norway (Evans et al. 2002), no palaeo-ice shelves appear to have been recognized in the geological record. Furthermore, only a few studies of modern ice-shelf moraines have been undertaken (Sugden & Clapperton 1981, Reynolds & Hambrey 1988; Glasser *et al.* 2006; Fitzsimons *et al.* 2012), so there is a need to characterize these features fully if new examples are to be discovered in the geological record.

The aim of this paper is to determine the composition and mode of formation of a moraine complex at the margin of the topographically constrained George VI Ice Shelf that is fed principally by the Antarctic Peninsula Ice Sheet. This ice shelf has previously been considered vulnerable to collapse (Luchitta & Rosanova 1998). By applying structural glaciological and sedimentological principles, the dynamics of the ice shelf and its impact on the landscape are determined, from which inferences are drawn about its dynamic behaviour. This

paper represents the most comprehensive analysis yet undertaken on how debris in an ice shelf is entrained and deposited.

Topographic, glaciological and geological setting of George VI Ice Shelf

Topography and glaciology

Since George VI Ice Shelf was first explored by the British Graham Land Expedition of 1934-37 (Stephenson & Fleming 1940), it has been the subject of numerous glaciological and geological investigations. It is the largest ice shelf on the west coast of the Antarctic Peninsula, covering an area of ~25,000 km^2 (Smith *et al*. 2007a,b), and measuring 450 km in length and 20 to 75 km in width (Holt *et al*. 2013) (Fig. 1A, inset). It occupies a deep, steep-sided composite trough ranging from 500 to 1000 m in depth (Maslanyj 1987). The trough extends beyond the ice shelf across the continental shelf of Marguerite Bay, and was evidently occupied by a major ice stream from the Antarctic Peninsula Ice Sheet at the Late Glacial Maximum (LGM) (Ó Cofaigh *et al.* 2005; Jamieson et al., 2012). Large outlet glaciers from the Antarctic Peninsula Ice Sheet are the biggest contributor to the ice shelf (Fig. 1B). The ice shelf is subject to melting in summer, when extensive surface lakes develop (Reynolds 1981) (Fig. 1A), and snow-free glacier ice is limited to the marginal zone adjacent to Alexander Island (Smith *et al.* 2013). The marginal zone in the vicinity of Ablation Lake and Moutonnée Lake, which is the subject of this investigation, was described by Stephenson & Fleming (1940) as an area of "pressure ice" extending about 2 km from land, disposed in a series of parallel ridges. These ridges are associated with an ice-shelf moraine, which Sugden & Clapperton (1981) interpreted as the product of thrusting. Ablation Lake and Moutonnée Lake are both epi-shelf lakes that have a direct hydraulic connection to the sea (Roberts *et al*. 2009).

George VI Ice Shelf has a strongly negative mass balance (Pritchard *et al.* 2012), and is receding rapidly from both ends (Holt *et al.* 2013). Most significant in terms of mass loss are high basal melt-rates induced by warm currents flowing

beneath the ice shelf (Jenkins & Jacobs 2008; Smith *et al*. 2013), but at least one area of localized basal freezing has been identified at Hobbs Pool (Pedley *et al*. 1988). Basal freezing leads to entrainment of sediment and has been suggested as a means whereby Palmer Land erratic material can be transferred to Alexander Island (Sugden & Clapperton 1980).

Unlike the more rapidly collapsing, relatively unconstrained ice shelves further north and west, George VI Ice Shelf is largely under compression. This compression is evident from the west- to northwest-directed flow across the Sound (Bishop & Walton 1981; Pearson & Rose 1983), and the form of the component flow units and structure derived from a Landsat multispectral scanner image from January 1973 (Reynolds & Hambrey 1988). From these data, it is evident that the ice adjacent to the Alexander Island shore originates from Palmer Land.

The complex flow regime gives rise to marked differences in thickness of the ice shelf (Fretwell *et al.* 2013). The thickest ice occurs in lobes extending from the grounding lines of the major outlet glaciers from Palmer Land, notably the Bertram Glacier (~275 m), Ryder Glacier (~250 m) and Goodenough Glacier (~400 m), whereas thicknesses are less adjacent to Alexander Island, especially near Ablation Point (~125 m) (Fig. 1B).

Geological context

George VI Ice Shelf occupies a major rift separating two distinct geological terranes (Bell & King, 1998; Vaughan & Storey (2000). Alexander Island is principally composed of (i) the sedimentary Jurassic-Cretaceous Fossil Bluff Group in the east, with minor mafic volcanic rocks (Macdonald et al., 1999), and (ii) the turbiditic Jurassic—Cretaceous LeMay Group in the west, which is an accretionary prism sequence (Burn 1984). The LeMay Group is unconformably overlain by Cretaceous—Palaeogene basaltic andesitic—rhyolitic volcanic rocks of the Alexander Island Volcanic Group (McCarron & Millar 1997). Plutonic rocks are also widespread in the north and far west (Care, 1983). By contrast, western Palmer Land is dominated by three principal rock groups: (i) basement rocks, Silurian in part, comprising orthogneiss, metapelite and minor marble, calc-silicate and

granulite that were metamorphosed to high-grade amphibolite facies in the Mesozoic Era (Harrison and Piercy, 1991); (ii) younger undeformed volcanic rocks consisting of Cretaceous mafic—intermediate lavas and pyroclastic rocks of the Antarctic Peninsula Volcanic Group, and Jurassic dacite—rhyolite ignimbrites and lavas of the Ellsworth Land Group (Hunter et al., 2006); and (iii) widespread Jurassic—Cretaceous plutons of the Antarctic Peninsula batholith (Leat et al., 1995), mainly granodiorites, tonalities and diorites, some of which have a foliated texture (Piercy and Harrison, 1991).

Quaternary glacial and associated sediments, largely attributed to the Last Glacial Maximum (LGM) or younger events, are distributed in the low-lying ice-free areas adjacent to the ice shelf (Clapperton & Sugden 1982; Bentley *et al.* 2005; Roberts et al., 2008). The Antarctic Peninsula Ice Sheet filled the Sound and extended out to the continental shelf edge at the LGM (Payne *et al.* 1989; Bentley *et al.* 2005, 2006, 2009; Davies *et al.* 2012). From the presence of Palmer Land erratics in ice-shelf moraines at elevations of 80-110 m.a.s.l., it is evident that the Peninsula Ice Sheet was probably much thicker at the LGM (Sugden & Clapperton 1980; Clapperton & Sugden 1982; Smith *et al.* 2007a). Sugden & Clapperton (1981) mapped and described ice-shelf moraines related to the modern ice shelf along its western margin, where they occur sporadically along a stretch of 150 km of Alexander Island coastline. Sediment cores and barnacles suggest that there were two periods during the Holocene Epoch when George VI Ice Shelf was absent from the Ablation Lake area (Smith *et al.* 2007b; Hjort *et al.* 2001).

Methods

Satellite remote sensing and aerial photography for overall ice-shelf structure and dynamics

A cloud-free Landsat ETM+ 7 scene from 13 February 2003 was used to map longitudinal and transverse flow features, flow-unit boundaries and internal structures in the Bertram Glacier/Ablation Lake sector of the George VI Ice Shelf at a scale of 1:100,000 using the structurally controlled lakes as a guide (Figs. 1A, 2A). A combination of a true-colour band combination (30 m pixel resolution) and

Landsat 7's panchromatic band (15 m pixel resolution) were selected as they offered the greatest spectral contrast between ice, snow, water and shadow on the surface of the ice shelf. Within the field area, ASTER VNIR Level 1B Multispectral satellite imagery from 13th February 2009 (15 m resolution; swath 60 km) was used to map exposed structures, and used as a basis for plotting field observations (Figs. 1A, 2B). The velocity data (Fig. 2A) for the Bertram Glacier/Ablation Lake segment of the ice shelf was obtained using Interferometric Synthetic Aperture Radar (Rignot *et al.* 2011).

Ice-structural mapping – foliation and fractures

Two main structures at the margin of the ice shelf were identified and recorded in the field: (i) a coast-parallel steeply dipping foliation (n=112) and (ii) a set of cross-cutting fractures orthogonal to the ice margin (n=93). Data are plotted on lower hemisphere equal-angle projections for two zones to accommodate change in the orientation of the coastline. Additional structures identified include isoclinal and similar folds and veins of clear ice cutting the dominant foliation. Although these were insufficiently abundant to undertake statistical analysis, they are important for resolving the structural history of the ice shelf.

Ice-shelf moraine morphology and sedimentology

In order to define the processes of ice-shelf moraine formation and to characterize the ice-shelf moraine landsystem, a range of standard sediment-analytical techniques and morphological analysis were utilized (Hubbard & Glasser 2005; Hambrey & Glasser 2012). Lithofacies are defined according to the proportions of mud, sand and gravel using a classification of poorly sorted sediments (Hambrey & Glasser 2003). Other specific attributes of lithofacies documented include: bedding characteristics; texture, including estimates of gravel component and particle-size analysis of the sand and finer fraction using a combination of sieving and a SediGraph 5100 analyser; clast morphology including Powers (1953) roundness and shape defined by measurements of a, b and c-axes on sets of 50 clasts, and analysed using triplots and the RA/C_{40} index method of Benn and Ballantyne (1994); and clast-surface features such as striations and facets. These lithofacies

were placed in the context of a series of eight transects measured from pre-modern ice-shelf terrain to ice-shelf bare ice across the moraine, approximately normal to the ice margin, using an Abney level and 30 m tape.

Clast provenance

The lithology of clasts sampled for sedimentological attributes was documented, with percentages of Alexander Island and Palmer Land clasts recorded. In addition, the full range of exotic and local clasts was sampled from the moraines adjacent to Ablation Lake (S) and Moutonnée Lake (N) and analysed using thin sections.

Analysis of ice-shelf dynamics in the Bertram Glacier sector

Ice flow in the Bertram Glacier/Ablation Lake sector is directed across the Sound towards the west and northwest. Ice velocity maps (Rignot *et al.* 2011) show that Bertram Glacier has two zones of faster flow, separated by an area of slower moving ice. The southern portion of Bertram Glacier (Bertram (I); Figs. 1A, 2B) crosses the Sound towards Ablation Lake. At its Palmer Land grounding-line, Bertram Glacier flows at ~420 m a^{-1}, gradually slowing to less than 20 m a^{-1} by the time it reaches Alexander Island, indicating that this portion of the ice shelf, like areas to the north and south, is under compression (Fig 2A).

Morphology of ice shelf and bordering moraines

Seven distinct morphological zones can be identified between the source ice stream from the Antarctic Peninsula Ice Sheet (Bertram Glacier), across the inner ice shelf, the “pressure ridges” adjacent to Alexander Island and the actively forming moraines, to the valley sides (Fig. 3A):

(i) *Palmer Land ice streams (Bertram Glacier in the sector studied)*.

From the Landsat imagery, surface features are dominated by a set of transverse crevasses and other intersecting crevasses, and a series of irregular troughs where inter-crevasse blocks have collapsed (Fig. 1A). As Bertram Glacier approaches George VI Ice Shelf, crevasses appear to be water-filled. Crevasses then close up and become draped by snow, surviving as crevasse traces.

(ii) *Ice-shelf surface (central)*. Broad smooth, snow-covered ridges and depressions containing elongate ponds, connected by supraglacial streams, characterize the bulk of the ice shelf. Relief is on a scale of several metres and the distance between ridge crests is typically >100 m. Dolines mark flow-unit boundaries and there are no crevasses.

(iii) *Ice-shelf surface (western margin)*. A zone of rough ice, 0.5 to 2 km wide, comprising a series of shore-parallel steep-sided ridges and troughs. Typically, these ridges are hundreds of metres long and have a relief of 10-15 m, and an amplitude of 50-200 m. Superimposed on this relief are metre-scale "ice ships" (pinnacles), which are differentially weathered along the coast-parallel foliation (Fig. 3B), as well as supraglacial streams, ponds and cryoconite holes containing well-sorted sand or mud. In the vicinity of Moutonnée Lake (Fig. 4), the ice shelf is prevented from encroaching into this embayment by a bedrock bar (*cf*. Ablation Lake, below). A vertical ice cliff across the mouth of the embayment rises some 20 m above the frozen lake surface, and is probably grounded on the lake bottom.

(iv) *Ice tongue (Ablation Lake).* A heavily fractured tongue of ice-shelf ice extends into the middle of the lake, pushing up lake ice into c. 5m-high pressure ridges.

(v) *Ice-cored moraine*. Two zones of debris characterize the edge of George VI Ice Shelf: active and ice-cored, and inactive with no apparent ice core ("old" degraded moraines; see (vi) below). Sediment sampling (Fig. 4), lithofacies descriptions and eight morphological transects (Fig. 5) were undertaken within these two zones (Fig. 5). The ice-cored moraine comprises a veneer of clast-rich sandy diamicton and sandy gravel, from a few centimetres to a few metres in thickness, overlying ice-shelf ice (Fig. 6A, B). This ice normally has a foliation that is near-vertical or steeply dipping shelf-wards. The ice-cored moraine has a relief of about 20 m, and some of the ridges are sharp-crested, especially where debris is actively ablating from the underlying ice. Ablation is by sublimation in the sub-zero conditions of early summer, and later by melting. Sediment sublimating from ridge crests is blocky, but collapses to form debris flows during periods of thaw. However, despite extensive debris cover, the amount of debris in the ice is low, typically <10 % by volume. The debris layers are parallel to the foliation (Fig. 3C). Boulders, commonly exceeding 1 m in diameter, are scattered over the ice-cored

moraine, and include many of granite and gneiss originating from Palmer Land. Ablation and undercutting in lakes produces unstable ice cliffs up to 5 m high, from which ice blocks topple.

(vi) *"Old" degraded moraines*. These inactive moraines are composed of sandy gravel and clast-rich sandy diamicton, and there is no sign of buried ice. In some places these moraines occur as former ice-contact benches up to 80 m above sea level. There is a "lag" of dispersed boulders on these surfaces, including Palmer Land erratics. Bedrock is only visible at the rock bar across the mouth of Moutonnée Lake.

(vii) *Cliffs and scree*. Actively forming scree and colluvium below cliffs of volcanic and sedimentary strata of the Fossil Bluff Formation (Jurassic-Cretaceous age) occur inland of the degraded moraines (Fig. 3A). Some angular boulders from this zone have fallen onto the moraines.

Structural glaciology of ice-shelf margin

Ice-shelf margin

The structural glaciology of the western margin of the ice-shelf, representing the distal reach of Bertram Glacier, was systematically mapped zone in (iii) above. This area coincided with the multiple shore-parallel ridges (Fig. 7) and strong near-vertical coast-parallel foliation. Numerous ice ships up to 2 m high are superimposed on these ridges (Fig. 3C), the morphology of which is controlled by differential weathering of different ice facies in the foliation.

Structural sequence

Exposed ice at the margin of the ice shelf reveals several intersecting sets of structures. Based on cross-cutting relationships the following structures (using standard structural geological notation) in order of formation can be discerned:

Foliation (S_1). Comprising coarse bubbly and fine ice, this structure is only found as remnants in the form of layers that have been isoclinally and similarly folded, of metre-scale amplitude. The marked thickening of ice layers in the hinge-zone and attenuation of the limbs is indicative of strong compressive deformation.

This structure is probably derived from the flow stripes, inherited from Bertram Glacier, and their continuation into the ice shelf. Folding (F_2) took place as the ice approached Alexander Island.

Foliation (S_2). This is the dominant structure observed in the ice-shelf margin, primarily comprising coarse bubbly ice and coarse clear ice, and aligned parallel to the ridges. (Fig. 7). Stereonets and eigenvalues indicate a strong near-vertical preferred orientation of this structure parallel to the coast (Fig. 7A). Locally, the dip of this structure declines to c. 45°at the ice edge. In the moraine zone (v) above), disseminated mud, sand and gravel of mixed lithologies (including exotic clasts) are found within some coarse clear layers, and this ablates out to produce the debris cover. The continuity of layering resembles types of arcuate foliation found below icefalls in valleys glaciers, which originate from the closure and healing of crevasses. This structure, containing continuous layers, differs from the normal anastomosing layers found in longitudinal foliation typical of valley glaciers, where individual layers can rarely be followed for more than a metre (Hambrey & Lawson 2000).

Sugden & Clapperton (1981) analysed the oxygen isotopic signature of these ice facies . They found that the coarse bubbly ice facies (their “white bubbly ice”) had a value of $\delta^{18}O$ of -18.12‰, whereas the coarse clear ice with debris had $\delta^{18}O$ values ranging from -14.93 to -9.88‰. The coarse bubbly ice is interpreted as glacier ice derived from firnification processes, and is supported by the lighter isotopic values of Sugden & Clapperton (1981). The coarse clear ice with heavier isotopic values is interpreted as frozen water-ice from transposed water-filled crevasses inherited from the heavily crevassed Bertram Glacier.

Strong compression as the ice impinges on Alexander Island results in pure shear and substantial modification of the former water-filled crevasses and inter-crevasse blocks of coarse bubbly ice. There is little evidence of simple shear as the ice approaches this margin. Plausible modes of debris entrainment are reactivation of crevasses as shear zones and folding of basal ice before Bertram Glacier enters the ice shelf.

Thrusts (S_3). No evidence of thrusting was found in the sectors mapped, although 3 km south of Moutonnée Valley, Sugden & Clapperton (1981) recorded

clear evidence of thrusting, notably displacements of several metres in the walls of an abandoned meltwater tunnel.

Fractures (S_4). Cracks in the ice surface have directionally variable orientations, but stereographic projections and eigenvalues indicate they are strongly orthogonal to the ice margin (Fig. 7B). The cracks are sharply defined, but are commonly anastomosing or cross-cutting. A few show bubble planes, but there are no veins of clear ice as is typical of crevasse traces. Rarely, cracks are open to a few centimetres width. As noted above, strong compression occurs with the principal compressive strain-rate acting perpendicular to the Alexander Island coast, whereas the cracks indicate extension parallel to the coast.

Open irregular crack (S_5). A single crack up to a metre or so wide runs approximately parallel to the coast, located roughly at the boundary between clean ice and the ice-cored moraine. It also runs through lake ice at Moutonnée Lake. This crack shows vertical displacements of half-a-metre maximum, but these vary during the course of the day. This open crack cuts across all other structures and is interpreted as a tide crack.

Ice-shelf sedimentology

The principal lithofacies associated with the ice-cored moraine at the edge of George VI Ice Shelf (zone v) are clast-rich sandy diamicton and sandy gravel (muddy), which grade into each other (Figs. 8, 9). Other minor lithofacies are sandy gravel (2 samples) and sand (2 samples), associated with supraglacial stream courses within the moraine and in clean ice areas respectively. The diamicton and sandy gravel (muddy) lithofacies are of basal derivation, melting out from the dominant foliation. Despite basal melting of the ice shelf (Smith *et al.* 2013), substantial Palmer Land debris forms part of these sediments. The moderately well-sorted sandy gravel is the product of debris flows derived from the above facies, but with fines winnowed out, or from more vigorous reworking by streams. The well-sorted sand has been transported by supraglacial streams, but is of aeolian derivation. The chief attributes of each lithofacies are presented in Figure

8, and representative sedimentological data in Figure 9. See Supplementary Material for a full facies analysis.

Provenance of clasts

Thin-section examination of clasts collected from the actively forming ice-shelf moraines between Ablation and Moutonnée lakes clearly define either a Palmer Land or a local Alexander Island provenance (Supplementary Data; Table S1). Arkose and rarer volcanilithic sandstone, derived from the Fossil Bluff Group, indicate an Alexander Island provenance. Some clasts contain distinctive chlorite-altered volcanic glass, a common Fossil Bluff Group characteristic (*cf*. Horne & Thomson, 1972). The prehnite-pumpellyite-grade metamorphism shown by the sandstones is consistent with the metamorphic grade of the Fossil Bluff Group (Miller and Macdonald, 2004). Plutonic rock clasts are tonalite and quartz diorite, with minor granite and diorite. They were derived from the Antarctic Peninsula batholith in northern Palmer Land. The plutonic rocks are distinguished from Palmer Land basement either by an absence or weak development of a tectonic fabric (foliation), or by minimal recrystallization. Clasts derived from Palmer Land basement consist of amphibolite, dioritic and tonalitic gneiss, and quartzose phyllite. They all show a strong textural foliation, including aligned biotite crystals and segregated bands dominated by different mineral proportions, and conspicuous marginal recrystallization of feldspar to quartzo-feldspathic mosaics; some also contain fine quartzo-feldspathic veins resembling mylonite. No outcrops of these lithologies occur on Alexander Island. The most distinctive basement clast lithology is a tonalite containing numerous large garnet crystals that is only found in Palmer Land in outcrops flanking Bertram Glacier. A Palmer Land source is thus preferred for all crystalline clasts, the proportion of which varies from 2 % to 20 % (Figs. 9, 10). Volcanic lithologies include mafic and intermediate lavas and hypabyssal intrusive rocks, and dacitic pyroclastic rocks. None is likely to have originated from Alexander Island as the volcanic outcrops are situated west of the main topographic

divide, with the possible exception of a small contribution from mafic lavas interbedded with the Fossil Bluff Formation. It is more likely that most were derived from Palmer Land, either from dykes or lavas within the Antarctic Peninsula Volcanic Group (mafic–intermediate) or the dacitic Ellsworth Land Volcanic Group.

Discussion

Dynamics of George VI Ice Shelf inferred from structural glaciology

Most ice shelves have flow-parallel features, commonly referred to as flow-lines or flow-stripes, which are inherited from the inland ice that supplies them (e.g. Crabtree & Doake 1980; Fahnestock *et al.* 2000; Glasser & Scambos, 2008; Glasser *et al.* 2009, 2011, in review; Holt 2013). Commonly, these features are visible even in areas of net accumulation. Where satellite imagery reveals exposed glacier ice and is further supplemented by ground observations, it has been demonstrated that these flow features are the surface manifestation of longitudinal foliation (Reynolds & Hambrey 1988; Hambrey 1991; Hambrey & Dowdeswell 1994; Glasser *et al*. in review). By analogy with valley glaciers with converging flow units, this longitudinal structure may be considered to be the product of folding of primary stratification; as flow converges into a distinct ice stream the ice becomes folded about flow-parallel axes, accompanied by attenuation of fold limbs and thickening of fold hinges as the ice undergoes simple shear (Hambrey & Glasser 2003). Recrystallization under simple shear further leads to transposition of the original layers to the extent that the new longitudinal structure replaces the primary stratification. This folding mechanism also explains how basal debris can be entrained into higher levels in a glacier (Hambrey & Glasser 2003).

George VI Ice Shelf differs from most ice shelves in being constrained; in this case within the long tectonic rift of George VI Sound (Crabtree *et al*. 1985), and in that extending flow with calving is only evident at the northern and southern extremities. In the central zone, where the fieldwork for this study was undertaken, the ice shelf is fed by Bertram Glacier, which from satellite imagery is

not only characterized by flow-stripes but also complex, predominantly transverse crevassing and large irregular rifts. The projection of both flow stripes and crevasses into the ice shelf is clearly visible, as sets of supraglacial lakes form parallel to the foliation (i.e. flow-stripes) and healed crevasses. Confirmation that these interpretations are correct is provided by exposed ice in the narrow zone where the Bertram Glacier flow unit impinges on Alexander Island. The longitudinal foliation (S_1) in Bertram Glacier, inferred from flow-stripes and associated supraglacial lakes, travels across the ice shelf rather than turning north towards the calving margin. However, it ceases to become visible in the imagery close to Alexander Island. This pattern of foliation transfer across the ice shelf is also evident where other ice streams flow into the ice shelf. Indeed, some this foliation is folded, indicating that the relationship of parallelism between flow direction and flow stripes breaks down. On the ground, in the vicinity of Ablation Lake, this structure has been deformed into tight similar or isoclinal folds, with axes parallel to the Alexander Island margin.

This first foliation (S_1), however, is largely over-printed by the crevasse-related features that formed near the lower reaches of Bertram Glacier, and give rise to a new foliation (S_2) perpendicular to the first one. This new foliation is the product of pure shear, arising from compressive flow as crevasses are healed and their traces are transposed as they cross the ice shelf. Any basal debris entrained within S_1 would be transposed into S_2. Satellite imagery confirms that many transverse crevasses in lower Bertram Glacier are water-filled, and, because of the resulting uneven topography, supraglacial lakes form parallel to this structure. By the time this structure reaches the Alexander Island margin at Ablation Lake, it is exposed, with varying proportions of coarse clear ice and coarse bubbly ice, steeply dipping inwards or aligned vertically. The isotopic contrast between coarse bubbly and coarse clear ice (Sugden & Clapperton 1981) also support a glacier ice and water ice origin respectively. With a lower albedo, the coarse clear ice preferentially melts faster, and therefore the high-relief topography at this margin is controlled by the crevasse trace-derived structure.

InSAR-derived velocities (Rignot *et al.* 2011) indicate that the ice in this central belt is under compression, with the maximum compressive stress acting

perpendicular to the axis of the ice shelf. Velocities decline from >400 m a^{-1} at the lower end of Bertram Glacier close to the grounding zone, to <100 m a^{-1} in the vicinity of Ablation Lake (Fig. 2A).

However, the above structural interpretation does not apply everywhere on the Alexander Island margin. In a wide-ranging survey of the ice margin and adjacent geomorphology, Sugden & Clapperton (1981) demonstrated that the crevasse trace-related foliation (S_2) was not always steeply dipping, but showed signs of distinct displacements, leading them to infer that this structure was a series of thrusts (S_3), with the topography being explained as a zone of "pressure ridges" rather than the product of differential ablation. Thus, there are at least two glaciotectonic processes operating as the ice impinges on Alexander Island, although thrusting may only be a localised mechanism.

Additional evidence of the deformation regime near Ablation Valley is the widespread formation or cracks orthogonal to the coast (S_4). To compensate for the compression that produces foliation (S_2), these cracks form perpendicular to it, and indicate extension parallel to the coast.

In summary, George VI Ice Shelf is supplied almost entirely from ice streams emanating from the interior of Palmer Land. Only in a few cases (Eros, Grotto, Jupiter/Haumea, Pluto and Mars glaciers) do Alexander Island's own glaciers extend into the ice shelf (Reynolds & Hambrey 1988), and never by more than a few kilometres. These confluence zones are also associated with ridges parallel to the prevailing crevasse trace-related foliation.

Significance of clast provenance

The contrasting geological terranes (domains) on either side of the Cenozoic rift of George VI Sound are reflected in the clasts of the ice-shelf moraine. The farthest travelled clasts are intrusive and metamorphic lithologies from western Palmer Land (Vaughan & Storey 2000). The clear provenance route shown by analysis of the clasts shows that they have been carried through Bertram Glacier, and reconstructing their potential flow paths inland to the last nunatak suggest a maximum transport distance of 100 km from the interior of the Antarctic Peninsula Ice Sheet. Conversely, incorporation of far-travelled metasedimentary clasts from

473 the Latady Group is unlikely, as the Group is restricted to southern and eastern
474 Palmer Land on the east-facing side of the main Palmer Land topographical divide
475 (Hunter & Cantrill, 2006). The roundness and shape characteristics of the
476 measured pebble-sized clasts indicate transport within the zone of traction at the
477 base of the ice stream. However, structural processes, notably folding to produce
478 the S_1 foliation, would allow basal debris to reach a high englacial position, thereby
479 becoming protected from basal melt in the ice shelf. Additionally, some large
480 boulders (> 1m) are angular, and these may have been derived from supraglacial
481 debris falling onto the accumulation area of Bertram Glacier, but soon becoming
482 buried by snow and following an englacial path, until released by ablation close to
483 Alexander Island.
484 The sedimentary, and possibly some mafic volcanic, clasts are locally
485 derived Fossil Bluff Formation lithologies of Alexander Island. These lithologies are
486 represented in the cliffs adjacent to the ice-shelf moraine, but their shape
487 characteristics indicate that the sediment is primarily of basal derivation, although
488 there are scattered clusters of single-lithology angular clasts that suggest a
489 shattered bedrock origin with minimal subglacial modification. There is little
490 evidence to suggest that the adjacent cliffs currently supply supraglacial material
491 to the moraine.
492 Overall, the fact that the proportion of Palmer Land clasts within the ice-
493 shelf moraine accounts for only 2 % to 20 % indicates that the bulk of the sediment
494 is entrained where the ice shelf becomes grounded as it impinges on the Alexander
495 Island shore. The exact process of entrainment could not be ascertained, however,
496 but tight folding is suspected in this zone of compression.
497
498 *Relationship between ice-shelf structure and moraine morphology*
499 The ice-shelf moraine comprises a series of irregular ridges of debris forming a thin
500 veneer over ice. The source of this debris is disseminated mud, sand and gravel in
501 the coarse clear layers in foliation (S_2). The absence of debris-rich ice suggests that
502 many tens of metres of ice need to have melted out to produce the amount of
503 sediment on the surface, which is typically a metre or more in thickness. The debris
504 melts out from near-vertical foliation, so is unable to maintain the form of the

original structure. It forms unstable ridges of sediment, which rapidly collapse and then undergo debris flowage during the melt-season. There is no evidence of the thrust-faulting mechanism advocated by Sugden & Clapperton (1981) in the production of these moraines. Moraine morphology reflects the internal structure composition of the ice shelf (foliation S_2) only to the extent of providing the source of the debris.

The character of the ice shelf moraines reported in this study therefore contrast with that of ice-shelf moraines around the McMurdo Ice Shelf (Ross Sea, Antarctica). The McMurdo moraines originate by accretion of older subglacial sediment on the sea floor as a result of basal freeze-on of marine waters, which is then released as gently inclined sheets on and adjacent to land (Glasser *et al.* 2006). However, these sheets of sediment also rapidly degrade, and the resulting moraines ultimately show few signs of these processes. Furthermore, both the George VI and McMurdo ice-shelf moraines are quite different from those produced by terrestrial glaciers, which are the product of a variety of different processes, such as thrusting (e.g. Hambrey *et al*. 1997, 1999; Bennett 2001; Lønne & Lauritsen 1996), delivery of debris to an active margin (e.g. Benn & Evans 2010; Bennett & Glasser, 2009; Lukas, 2005) or ice stagnation (Evans 2003). Of these, the closest terrestrial analogue for the George VI ice shelf moraines is where "controlled moraines" are formed, such as in the High-Arctic. Evans (2009) described such moraines as forming in linear fashion from internal debris layers to produce hummocky moraine.

Preservation potential of ice-shelf moraines

The Ablation Lake area of Alexander Island is an area of net ablation, but the contemporary ice-shelf moraines show little sign that the ice-shelf surface is lowering. The low debris concentrations in S_2 foliation suggest that accretion of debris is slow, but no time-series data are available to quantify the rate. The moraine debris is thin and subject to levelling by debris-flowage, so the resulting landforms are likely to be subdued features. This is confirmed by the presence of

537 "old" higher-level ice-shelf moraines, which are represented by smooth benches
538 and metre-scale ridges. Similarly, moraines associated with the southern McMurdo
539 Ice Shelf are ice-dominated, and are also likely to produce subdued bench-like
540 features. This paper provides a detailed description of an ice-shelf moraine for the
541 first time, and this can be used as a basis for locating such features in the
542 geological record. Such features have already been identified in the Canadian
543 Arctic (England *et al.* 1978, 2009; Hodgson et al. 1984) and northern Norway
544 (Evans et al. 2002), but there is no reason to suppose that they are not more
545 widespread. The key identifiers are near horizontal benches underlain by poorly
546 sorted sediment, together with a scatter of local and far-travelled ice-transported
547 boulders on the surface.
548
549 *Conceptual model of ice-shelf moraine formation*
550 By following the structures developed in Bertram Glacier in Palmer Land across the
551 ice shelf, the dynamic regime and mode of debris entrainment can be summarized
552 in a conceptual diagram (Fig. 11). Bertram Glacier incorporates igneous and
553 metamorphic debris from Palmer Land.
554 Two mechanisms appear possible to allow debris from Palmer Land to
555 travel right across the George VI ice shelf. Firstly, to protect basal debris from
556 melting out as it enters marine waters, basal freeze-on would have occurred in the
557 past, despite the rapid sub-ice shelf melting that is taking place today (Jenkins &
558 Jacobs 2008; Smith *et al*. 2013). Freeze-on may have occurred where meltwater
559 from the fast-flowing ice stream came into contact with the saline water at a
560 slightly lower temperature. The validity of this process is confirmed by the
561 recognition of at least one area of localized basal freezing, at Hobbs Pool in Palmer
562 Land, 64 km to the south (Pedley *et al*. 1988).
563 Secondly, basal debris could have been folded into a high englacial position
564 in Bertram Glacier, and therefore remained out of reach of basal melting processes
565 in the ice shelf. Recumbent folding at the base of a glacier (Hudleston 1976), or
566 upright folding with flow-parallel axes (Hambrey et al. 1999), are common
567 processes for elevating basal debris in polythermal ice masses. Given the
568 relationships between the two foliations, it seems that the second process is the

569 most plausible for delivering Palmer Land debris to Alexander Island: basal debris
570 was folded within stratified ice in a grounded zone of flow convergence, becoming
571 aligned parallel to S_1 and then transposed into the plane of foliation S_2 as the ice
572 became compressed against Alexander Island. A third possible alternative
573 mechanism, whereby a grounded Bertram Glacier formerly extended across
574 George VI Sound, is discounted because a central submarine bedrock ridge would
575 have diverted ice to the north or south.
576
577

578 Conclusions

579 This investigation provides insights concerning the dynamics and structural
580 evolution of an ice shelf strongly constrained by topography. Analyses of ice
581 dynamics then informs how debris is entrained and deposited to form an ice-shelf
582 moraine. The key conclusions are as follows:
583 (1) George VI Ice Shelf is nourished primarily by large ice streams
584 emanating from the Antarctic Peninsula Ice Sheet. Analysis of satellite radar
585 altimetry data indicates that the ice shelf thins from east to west, and that the
586 velocity also declines in this direction. This central part of the ice shelf is under
587 strong compression in the flow direction.
588 (2) Linear structures within the ice shelf are crevasse traces and foliation
589 inherited from Palmer Land outlet glaciers; these structures are defined by the
590 distribution of supraglacial lakes.
591 (3) The dominant structure exposed at the ice surface adjacent to
592 Alexander Island is a coast-parallel foliation (S_2) derived from water-filled crevasses
593 in lower Bertram Glacier. An earlier foliation (S_1) is strongly folded, reflecting
594 strong compression at this margin. Local thrusting (S_3) was recorded beyond the
595 field area (Sugden & Clapperton, 1981). All these structures are intersected at right
596 angles by closely spaced fractures (S_4), few of which are open.
597 (4) A belt of moraine lies on the ice shelf closest to the shore. Varying in
598 height and thickness, the moraine consists of basally derived debris, with up to 20
599 % of clasts derived from Palmer Land. Given that the ice shelf experiences

600 substantial basal melting, the initial entrainment process was probably by folding
601 of the basal layer into a high englacial position, which can occur where ice-flow in
602 wide accumulation zones becomes more constrained.
603 (5) The morphology of the ice-shelf moraine reflects the alignment of the S_2
604 foliation, but debris-flowage overprints this in many places. Ridges with the
605 highest elevations reflect higher concentrations of debris in the ice, but their
606 collapse with debris flowage into depressions results in topographic inversion.
607 These ridges represent a close analogue of "controlled moraines" (Evans 2009), as
608 described for terrestrial Arctic glaciers.
609 (6) As indicated by older ice-shelf moraines, the preservation of these
610 forms is subtle but distinctive. Their attributes are near horizontal benches
611 underlain by poorly sorted sediment, together with a scatter of erratics on the
612 surface. The ridges collapse into low-relief benches on adjacent hillsides, underlain
613 by basal till. As such, they may be more widespread than hitherto recognized in
614 areas affected by Pleistocene ice sheets.
615
616

Acknowledgements

This paper is an outcome of the project "Glacial history of the NE Antarctic Peninsula Region over centennial to millennial timescales", funded by the Natural Environment Research Council, Antarctic Funding Initiative (Grant no: NE/F012896/1). We thank the British Antarctic Survey and their staff in Cambridge and at Rothera Station, Antarctica, for excellent logistical support. We acknowledge especially our field assistant, Ian Hey, for organising the field logistics and helping with the field campaign.

Project design was by NFG, with contributions from MJH, BJD, JLS and JLC. The fieldwork was undertaken by MJH and BJD in November-December 2012. TOH undertook the satellite image analysis and JLS described thin sections of clasts for provenance. The paper was largely written by MJH, with contributions from all authors. We thank David Sugden and David Evans for their helpful and perceptive comments on this paper.

References

BELL, A. C. & KING, E. C. 1998. New seismic data support Cenozoic rifting in George VI Sound, Antarctic Peninsula. *Geophysical Journal International*, **134**, 889-902.

BENN, D. I. & BALLANTYNE, C. K. 1994. Reconstructing the transport history of glacigenic sediments: a new approach based on the covariance of clast shape indices. *Sedimentary Geology*, **91**, 215-227.

BENN, D. I. & EVANS, D. J. A. 2010. *Glaciers and Glaciation*. 2nd edition. Abingdon, UK: Hodder Education.

BENNETT, M. R. 2001.The morphology, structural evolution and significance of push moraines. *Earth Science Reviews,* **53***,* 197–236.

BENNETT, M. R. & GLASSER, N. F. 2009. *Glacial geology: ice sheets and landforms*, 2nd Edn. John Wiley & Sons, Chichester.

BENTLEY, M. J., HODGSON, D. A., SUGDEN, D. E., ROBERTS, S. J., SMITH, J. A., LENG, M. J. & BRYANT, C. 2005. Early Holocene retreat of the George VI Ice Shelf, Antarctic Peninsula. *Geology*, **33**, 173-176.

BENTLEY, M. J., FOGWILL, C. J., KUBNIK, P. W. & SUGDEN, D. E. 2006. Geomorphological evidence and cosmogenic $^{10}Be/^{26}AL$ exposure ages for the Last Glacial Maximum and deglaciation of the Antarctic Peninsula Ice Sheet. *GSA Bulletin*, **118**, 1149-1159.

650 BENTLEY, M. J., HODGSON, D. A., SMITH, J. A., Ó Cofaigh, C., Domack, E. W., Larter, R. D.,
651 Roberts, S. J., Brachfield, S., Leventer, A., Hjort, C., Hillenbrand, C.-D. & Evans, J. 2009.
652 Mechanisms of Holocene palaeoenvironmental change in the Antarctic Peninsula
653 region. The Holocene, 19, 51-69.
654 BENTLEY, M. J., FOGWILL, C. J., KUBIK, P. W. & SUGDEN, D. E. 2014. Geomorphological evidence
655 and cosmogenic 10Be/26Al exposure ages for the Last Glacial Maximum and
656 deglaciation of the Antarctic Peninsula Ice Sheet. *GSA Bulletin*, **118**, 1149-1159.
657 BISHOP, J. F. & WALTON, J. L. W. 1981. Bottom melting under George VI Ice Shelf, Antarctica.
658 *Journal of Glaciology*, **27**, 429-447.
659 BRITISH ANTARCTIC SURVEY 1982. *Geological Map, scale 1:5000,000, Northern Palmer Land.*
660 *BAS 500G, Sheet 5, Edn. 1*. Cambridge, British Antarctic Survey.
661 BURN, R. W. 1984. The geology of the LeMay Group, Alexander Island. *British Antarctic*
662 *Survey Bulletin*, **53**, 175-193.
663 CARE, B. W. 1983. The petrology of the Rouen Mountains, northern Alexander Island.
664 *British Antarctic Survey Bulletin*, **52**, 63-86.
665 CLAPPERTON, C. M. & SUGDEN, D. E. 1982. Late Quaternary glacial history of George VI Sound
666 area, West Antarctica. *Quaternary Research*, **18**, 243-267.
667 COOK, A. J. & VAUGHAN, D. G. 2010. Overview of areal changes of the ice shelves on the
668 Antarctic Peninsula over the past 50 years. *The Cryosphere*, **4**, 77-98.
669 COOK, A. J., Fox, A. J., VAUGHAN, D. G. & FERRIGNO, J. G. 2005. Retreating glacier fronts on
670 the Antarctic Peninsula over the past half-century. *Science*, **308**, 541-544.
671 CRABTREE, R. D. & DOAKE, C. S. M. 1980. Flow lines on Antarctic ice shelves. *Polar Record*, **20**,
672 31-37.
673 CRABTREE, R. D., STOREY, B. C. & DOAKE, C. S. M., 1985. The structural evolution of George VI
674 sound, Antarctic Peninsula. *Tectonophysics*, **114**, 431-442.
675 DAVIES, B. J., HAMBREY, M. J., SMELLIE, J. S., CARRIVICK, J. L. & GLASSER, N. F. 2012. Antarctic
676 Peninsula Ice Sheet evolution during the Cenozoic Era. *Quaternary Science Reviews,* **31**,
677 30-66.
678 ENGLAND, J. 1999. Coalescent Greenland and Innuitian ice during the Last Glacial
679 Maximum: revising the Quaternary of the Canadian High Arctic. *Quaternary Science*
680 *Reviews*, **18**, 421-456.
681 ENGLAND, J., BRADLEY, R. S. & MILLER, G. H. 1978. Former ice shelves in the Canadian High
682 Arctic. *Journal of Glaciology*, **20**, 393-404.

683 ENGLAND, J. H., FURZE, M. F. A. & DOUPÉ, J. P. 2009. Revision of the NW Laurentide Ice Sheet:
684 implications for paleoclimate, the northeast extremity of Beringia, and Arctic Ocean
685 sedimentation. *Quaternary Science Reviews*, **28**, 1573–1596
686 EVANS , D. J. A., 2003. Ice-marginal terrestrial landsystems: active temperate glacier
687 margins. *In* Evans, D. J. A. (ed) *Glacial Landsystems,* Arnold, London, pp. 259-288.
688 EVANS, D. J. A., 2009. Controlled moraines: origins, characteristics and palaeoglaciological
689 implications. *Quaternary Science Reviews*, **28**, 183-208.
690 EVANS, D. J. A., REA, B. R., HANSOM, J. D. & WHALLEY, W. B. 2002. Geomorphology and style of
691 plateau icefield deglaciation in fjord terrains: the example of Troms-Finnmark, north
692 Norway. *Journal of Quaternary Science*, **17**, 221–239.
693 FAHNESTOCK, M. A., SCAMBOS, T. A., BINDSCHADLER, R. A. & KVARAN, G. 2000. A millennium of
694 variable ice flow recorded by the Ross Ice Shelf, Antarctica. *Journal of Glaciology*,
695 **46**, 652-664.
696 FITZSIMONS, S. J., MAGER, S., FREW, R., CLIFFORD, A. & WILSON, G. 2012. Formation of ice-shelf
697 moraines by accretion of sea water and marine sediment at the southern margin of the
698 McMurdo Ice Shelf, Antarctica. *Annals of Glaciology*, **53**, 211-220.
699 FRETWELL, P. & 59 others 2013. Bedmap2: improved ice bed, surface and thickness datasets
700 for Antarctica. *The Cryosphere,* **7**, 375–393.
701 GLASSER, N. F. & SCAMBOS, T. A. 2008. A structural glaciological analysis of the 2002 Larsen B
702 Ice-Shelf collapse. *Journal of Glaciology*, **54**, 3-16.
703 GLASSER, N., GOODSELL, B., COPLAND, L. & LAWSON, W. 2006. Debris characteristics and ice-
704 shelf dynamics in the ablation region of the McMurdo Ice Shelf, Antarctica. *Journal of*
705 *Glaciology*, **52**, 223-234.
706 GLASSER, N. F., KULESSA, B., LUCKMAN, A., JANSEN, D., KING, E. C., SAMMONDS, P. R., SCAMBOS, T.
707 A., & JEZEK, K. C. 2009. Surface structure and stability of the Larsen C Ice Shelf, Antarctic
708 Peninsula. *Journal of Glaciology*, **55**, 400-410.
709 GLASSER, N. F., SCAMBOS, T. A., BOHLANDER, J., TRUFFER, M., PETTIT, E., & DAVIES, B. J. 2011. From
710 ice-shelf tributary to tidewater glacier: Continued rapid recession, acceleration and
711 thinning of Röhss Glacier following the 1995 collapse of the Prince Gustav Ice Shelf,
712 Antarctic Peninsula. *Journal of Glaciology*, **57**, 397-406.
713 GLASSER, N. F., JENNINGS, S. J., HAMBREY, M. J. & HUBBARD, B. in review. *Earth Surface*
714 *Dynamics*.

GRAHAM, A. G. C. & SMITH, J. A. 2012. Palaeoglaciology of the Alexander Island ice cap, western Antarctic Peninsula, reconstructed from marine geophysical and core data. *Quaternary Science Reviews*, **35**, 63-81.

HAMBREY, M. J., 1991. Structure and dynamics of the Lambert Glacier-Amery Ice Shelf system: implications for the origin of Prydz Bay sediments. *In* BARRON, J., LARSEN, B. et al. *Proceedings of the Ocean Drilling Program, Sci. Results,* Vol. 119, College Station, Texas, pp. 61-76.

HAMBREY, M. J. & DOWDESWELL, J. A. 1994. Flow regime of the Lambert Glacier-Amery Ice Shelf System, Antarctica: structural evidence from satellite imagery. *Annals of Glaciology,* **20**, 401-406.

HAMBREY, M. J. & GLASSER, N. F. 2003. The role of folding and foliation development in the genesis of medial moraines: examples from Svalbard glaciers. *Journal of Geology*, **111**, 471-485.

HAMBREY, M. J. & GLASSER, N. F. 2003. Glacial sediments: processes, environments and facies. *In* Middleton, G.V. (ed.) *Encyclopedia of Sediments and Sedimentary Rocks*. Dordrecht: Kluwer, 316-331.

HAMBREY, M. J. & GLASSER, N. F. 2012. Disciminating glacier thermal and dynamic regimes in the sedimentary record. *Sedimentary Geology*, **251-252**, 1-33.

HAMBREY, M. J. & LAWSON, W. J. 2000. Structural styles and deformation fields in glaciers: a review. *In* MALTMAN, A. J., HUBBARD, B. & HAMBREY, M. J. (eds.) *Deformation of Glacial Materials*. *Special Publication, Geological Society of London*, **176**, pp. 59-83.

HAMBREY, M. J., HUDDART, D., BENNETT, M. R. & GLASSER, N. F. 1997. Dynamic and climatic significance of "hummocky moraines": evidence from Svalbard and Britain. *Journal of the Geological Society,* **154**, 623-632.

HAMBREY, M. J., BENNETT, M. R., DOWDESWELL, J. A., GLASSER, N. F. & HUDDART, D. 1999. Debris entrainment and transfer in polythermal valley glaciers. *Journal of Glaciology,* **45**, 69-86.

HARRISON, S. M. & PIERCY, B. A. 1991. Basement gneisses in north-western Palmer Land: further evidence for pre-Mesozoic rocks in Lesser Antarctica. In: THOMSON, M. R. A., CRAME, J. A. AND THOMSON, J. W. (eds) *Geological evolution of Antarctica*. Cambridge University Press, Cambridge, 341-344.

HEYWOOD, R. B. 1977. A limnological survey of the Ablation Point area, Alexander Island, Antarctica. *Philosophical Transactions of the Royal Society of London*, **B279**, 39-54.

HILLENBRAND, C.-D., LARTER, R. D., DOWDESWELL, J. A., EHRMANN, W., Ó COFAIGH, C., BENETTI, S., GRAHAM, A. G. C. & GROBE, H. 2010. The sedimentary legacy of a palaeo-ice stream on the shelf of the southern Bellingshausen Sea: clues to West Antarctic glacial history during the Late Quaternary. *Quaternary Science Reviews*, **29**, 2741-2763.

HJORT, C., BENTLEY, M. J. & INGÓLFSSON, Ó. 2001. Holocene and pre-Holocene temporary disappearance of the George VI Ice Shelf, Antarctic Peninsula. *Antarctic Science*, **13**, 296-301.

HODGSON, D. A. 1994. Episodic ice streams and ice shelves during retreat of the northwesternmost sector of the late Wisconsinan Laurentide Ice Sheet over the central Canadian Arctic Archipelago. *Boreas*, **23**, 14–28.

HODGSON, D. A. & VINCENT, J.-S. 1984. A 10,000 yr. BP extensive ice shelf over Viscount Melville Sound, Arctic Canada. *Quaternary Research*, **22**, 18–30.

HOLT, T. O., GLASSER, N. F., QUINCEY, D. J. & SIEGFRIED, M. R. 2013. Speedup and fracturing of George VI Ice Shelf, Antarctic Peninsula. *The Cryosphere*, **7**, 797-816.

HORNE, R. R. & THOMSON, M. R. A. 1972. Airborne and detrital volcanic material in the Lower Cretaceous sediments of south-eastern Alexander Island. *British Antarctic Survey Bulletin*, **29**, 103-111.

HUBBARD, B. & GLASSER, N. F. 2005. *Field Techniques in Glaciology and Glacial Geomorphology*. Wiley, Chichester.

HUDLESTON, P. J., 1976. Recumbent folding at the base of the Barnes Ice Cap, Baffin Island, Northwest Territories, Canada. *Geological Society of America Bulletin*, **87**, 1684-1692.

HUNTER, M .A. & Cantrill, D. J., 2006. A new stratigraphy for the Latady Basin, Antarctic Peninsula: Part 2, Latady Group and basin evolution. *Geological Magazine*, **143**, 797-819.

HUNTER, M. A., RILEY, T. R., CANTRILL, D. J., FLOWERDEW, M. J. & MILLAR, I. L. 2006. A new stratigraphy for the Latady Basin, Antarctic Peninsula: Part 1, Ellsworth Land Volcanic Group. *Geological Magazine*, **143**, 777-796.

JAMIESON, S. S. R., VIELI, A., LIVINGSTONE, S. J., Ó COFAIGH, C.,. STOKES, C. R., HILLENBRAND, C-D. & DOWDESWELL, J. A. 2012, Ice stream stability on a reverse bed slope. *Nature Geoscience*, **5**, 799-802.

JENKINS, A. & JACOBS, S. 2008. Circulation and melting beneath George VI Ice Shelf, Antarctica. *Journal of Geophysical Research*, **113**, C04013, 10.1029/2007jc004449

JOHNSON, J. S., EVEREST, J. D., LEAT, P. T., GOLLEDGE, N. R., ROOD, D. H. & STUART, F. M. 2012. The deglacial history of NW Alexander Island, Antarctica, from surface exposure dating. *Quaternary Research*, **77**, 273-280.

LEAT, P. T., SCARROW, J. H. & MILLAR, I. L. 1995. On the Antarctic Peninsula Batholith. *Geological Magazine*, **132**, 399-412.

LØNNE, I. & LAURITSEN, T. 1996. The Architecture of a Modern Push-Moraine at Svalbard as Inferred from Ground-Penetrating Radar Measurements. *Arctic and Alpine Research*, **28**, 488-495.

LUCHITTA, N. K. & ROSANOVA, C. E., 1998. Retreat of northern margins of George VI and Wilkins ice shelves, Antarctic Peninsula. *Annals of Glaciology*, **27**, 41-46.

LUKAS, S. 2005. A test of the englacial thrusting hypothesis of 'hummocky' moraine formation: case studies from the northwest Highlands, Scotland. *Boreas*, **34**, 287-307.

MACDONALD, D. I. M.. LEAT, P. T., DOUBLEDAY, P. A. & KELLY, S. R. A. 1999. On the origin of fore-arc basins: new evidence of formation by rifting from the Jurassic of Alexander Island, Antarctica. *Terra Nova*, **11**, 186-193.

MASLANYJ, M. P. 1987. Seismic bedrock depth measurements and the origin of George-VI Sound, Antarctic Peninsula. *British Antarctic Survey Bulletin*, **75**, 51-65.

MCCARRON, J. J. & MILLAR, I. L. 1997. The age and stratigraphy of fore-arc magmatism in Alexander Island. *Geological Magazine*, **134**, 507-522.

MILLER, S. & MACDONALD, D. I. M. 2004. Metamorphic and thermal history of a fore-arc basin: the Fossil Bluff Group, Alexander Island, Antarctica. *Journal of Petrology*, **45**, 1453-1465.

MORRIS, E. M. & VAUGHAN, A. P. M. 2003. Spatial and temporal variation of surface temperature on the Antarctic Peninsula and the limit of viability of ice shelves. *In* DOMACK, E. W., LEVENTER, A., BURNETT, A., BINDSCHADLER, R., CONVEY, P., KIRBY, M. (eds), *Antarctic Peninsula climate variability: historical and palaeoenvironmental perspectives*. American Geophysical Union, Antarctic Research Series, Volume 79, Washington, D.C., 61-68.

Ó COFAIGH, C., DOWDESWELL, J. A., ALLEN, C. S., HIEMSTRA, J. F., PUDSEY, C. J., EVANS, J. & EVANS, D. J. A. 2005. Flow dynamics and till genesis associated with a marine-based Antarctic palaeo-ice stream. *Quaternary Science Reviews*, **24**, 709-740.

PAYNE, A. J., SUGDEN, D. E. & CLAPPERTON, C. M. 1989. Modelling the growth and decay of the Antarctic Peninsula Ice Sheet. *Quaternary Research*, **24**, 709-740.

PEARSON, M. R. & ROSE, I. H. 1983. The dynamics of George VI Ice Shelf, *British Antarctic Survey Bulletin*, 52, 205-220.

PEDLEY, M., PAREN, J. G. & POTTER, J. R. 1988. Local basal freezing within George VI Ice Shelf. *Journal of Glaciology*, **34**, 71-77.

PIERCY, B. A. & HARRISON, S. M. 1991 Mesozoic metamorphism, deformation and plutonism in the southern Antarctic Peninsula: evidence from north-western Palmer Land. *In* THOMSON, M. R. A., *et al*. (eds) *Geological evolution of Antarctica*. Cambridge University Press, Cambridge, 381-385.

POWERS, M. C. 1953. A new roundness scale for sedimentary particles. *Journal of Sedimentary Petrology,* **23**, 117-119.

PRITCHARD, H. D. & VAUGHAN, D. G. 2007. Widespread acceleration of tidewater glaciers on the Antarctic Peninsula. *Journal of Geophysical Research – Earth Surface*, **112**, 1–10.

REBESCO, M., DOMACK, E., ZGUR, F., LAVOIE, C., LEVENTER, A., BRACHFELD, S., WILLMOTT, V., HALVERSON, G., TRUFFER, M., SCAMBOS, T., SMITH, J. & PETTIT, E. 2014. Boundary condition of grounding lines prior to collapse, Larsen-B Ice Shelf, Antarctica. *Science*, 345, 1354-1358.

REYNOLDS, J. M. 1981. Lakes on George VI Ice Shelf, Antarctica. *Polar Record*, **20**, 425-432.

REYNOLDS, J. M. & HAMBREY, M. J. 1988. The structural glaciology of George VI Ice Shelf, Antarctic Peninsula. *British Antarctic Survey Bulletin*, **79**, 79-95.

RIGNOT, E., MOUGINOT, B. & SCHEUCHL, B. 2011. Ice flow of the Antarctic Ice Sheet. *Science*, **341**, 266-270.

RIGNOT, E., JACOBS, S., MOUGINOT, B. & SCHEUCHL, B. 2013. Ice-shelf melting around Antarctica. *Science*, **333**, 1427-1430.

ROBERTS, S. J., HODGSON, D. A., BENTLEY, M. J., SMITH, J. A., MILLAR, I. L., OLIVE, V. & SUGDEN, D. E. 2008. The Holocene history of George VI Ice Shelf, Antarctic Peninsula from clast-provenance analysis of epi-shelf lake sediments. *Palaeogeography, Palaeoclimatology and Palaeoecology*, 259, 258-283.

SMITH, J. A., BENTLEY, M. J., HODGSON, D. A. & COOK, A. J. 2007a. George VI Ice Shelf: past history, present behaviour and potential mechanisms for future collapse. *Antarctic Science*, **19**, 131-142.

SMITH, J. A., BENTLEY, M. J., HODGSON, D. A., ROBERTS, S. J., LENG, M. J., LLOYD, J. M., BARRETT, M. S., BRYANT, C. L. & SUGDEN, D. E. 2007b. Oceanic and atmospheric forcing of early Holocene ice shelf retreat, George VI Ice Shelf, Antarctic Peninsula. *Quaternary Science Reviews*, **26**, 500-516.

STEPHENSON, A. & FLEMING, W. L. S. 1940. King George the Sixth Sound. *Geographical Journal*, **96**, 153-164.

SUGDEN, D. E. & CLAPPERTON, C. M. 1980. West Antarctic Ice Sheet fluctuations in the Antarctic Peninsula area. *Nature*, 286: 378-381.

SUGDEN, D. E. & CLAPPERTON, C. M. 1981. An ice-shelf moraine, George VI Sound, Antarctica. *Annals of Glaciology*, **2**, 135-141.

TALBOT, M. H. 1988. Oceanic environment of George VI Ice Shelf, Antarctic Peninsula. *Annals of Glaciology*, **11**,161-164.

VAUGHAN, D. G. & DOAKE, C. S. M. 1996. Recent atmospheric warming and retreat of ice shelves on the Antarctic Peninsula. *Nature*, **379**, 328–331.

VAUGHAN, A. P. M. & STOREY, B. C. 2000. The eastern Palmer Land shear zone: a new terrane accretion model for the Mesozoic development of the Antarctic Peninsula. *Journal of the Geological Society*, **157**, 1243-1256.

Figure captions

1. The central part of George VI Ice Shelf, SW Antarctic Peninsula. (A) Landsat ETM+ 7 scene from 13 February 2003. The linear black areas on the ice shelf are structurally controlled surface lakes. (B) Ice-thickness data of ice shelf and source ice streams. Names refer to principal glacier flow-units.
2. Dynamics and structure of central George VI Ice Shelf. (A) InSAR-derived velocity distribution (Rignot et al. 2011). (B) Structural map of longitudinal structures (foliation) and transverse structures (crevasse traces, transposing to coast-parallel foliation), and flow-unit boundaries, based on the distribution of elongated lakes.
3. Ice-shelf morphology. (A) Overview of ice shelf moraines and Ablation Lake from the air; (B) debris layers forming ice-shelf moraine in ice cliff between Ablation Lake and Moutonnée Lake; (C) pinnacles and "ice ships" whose morphology is controlled by foliation and differential weathering
4. Location of transects normal to the ice margin between Ablation Lake and Moutonnée Lake, and sediment locations in ice-shelf moraine.
5. Transects through ice-cored ice-shelf moraine indicating thickness and facies distribution (see Fig. 4 for location).
6. Ice-shelf moraine morphology: (A) drape of diamicton overlying strongly foliated ice with minor debris near Ablation Lake; (B) ridge of sandy gravel at ice-shelf margin 500 m south of Moutonnée Lake.
7. Structural glaciological maps of zone between Ablation Lake and Moutonnée Lake, Alexander Island, showing (A) foliation and (B) fractures. Two sectors of uniform foliation orientation are defined, with accompanying stereographic (lower hemisphere, equal-angle) projections for each sector and each structure, together with eigenvalues. Transects for morphology (A to F) are indicated.
8. Principal lithofacies associated with ice-shelf moraine and adjacent foliated glacier ice. Relative abundance indicated from * (least) to ***** (most). Clast roundness: R = rounded, SR = subrounded; SA = subangular; A = angular. Sample numbers in bold refer to representative sedimentological data in

911 Figure 9; numbers in italics represent the full data-set in *Supplementary*
912 *Material,* Figure S4. Sample locations are illustrated in Figure 4.
913 9. Sedimentological data from ice-cored moraine. Column A - clast shape with a,
914 b and c-axis ratio plotted on a triangular diagram. Column B – histograms of
915 clast roundness. Column C – particle-size distribution of matrix in poorly
916 sorted lithofacies. Column D: relative proportions of exotic (Palmer Land) and
917 local (Alexander Island) clasts. Size of clast samples = 50. Diagram E – RA/C40
918 plot of data from poorly sorted lithofacies. Diagram F – cumulative particle-
919 size distribution graphs for principal lithofacies.
920 10. Palmer Land erratics within modern actively forming ice-shelf moraine on
921 Alexander Island. (A) Angular block of granite, surrounded by diamicton. (B)
922 subangular boulder of gneiss and muddy sandy gravel/diamicton emerging
923 from foliated ice.
924 11. Conceptual model of ice-shelf-moraine formation for George VI Ice Shelf,
925 showing transition from grounded ice on Palmer Land to the floating ice-shelf
926 reach, and its impingement on Alexander Island. Circles show details of
927 inferred structural relationships.
928
929
930
931

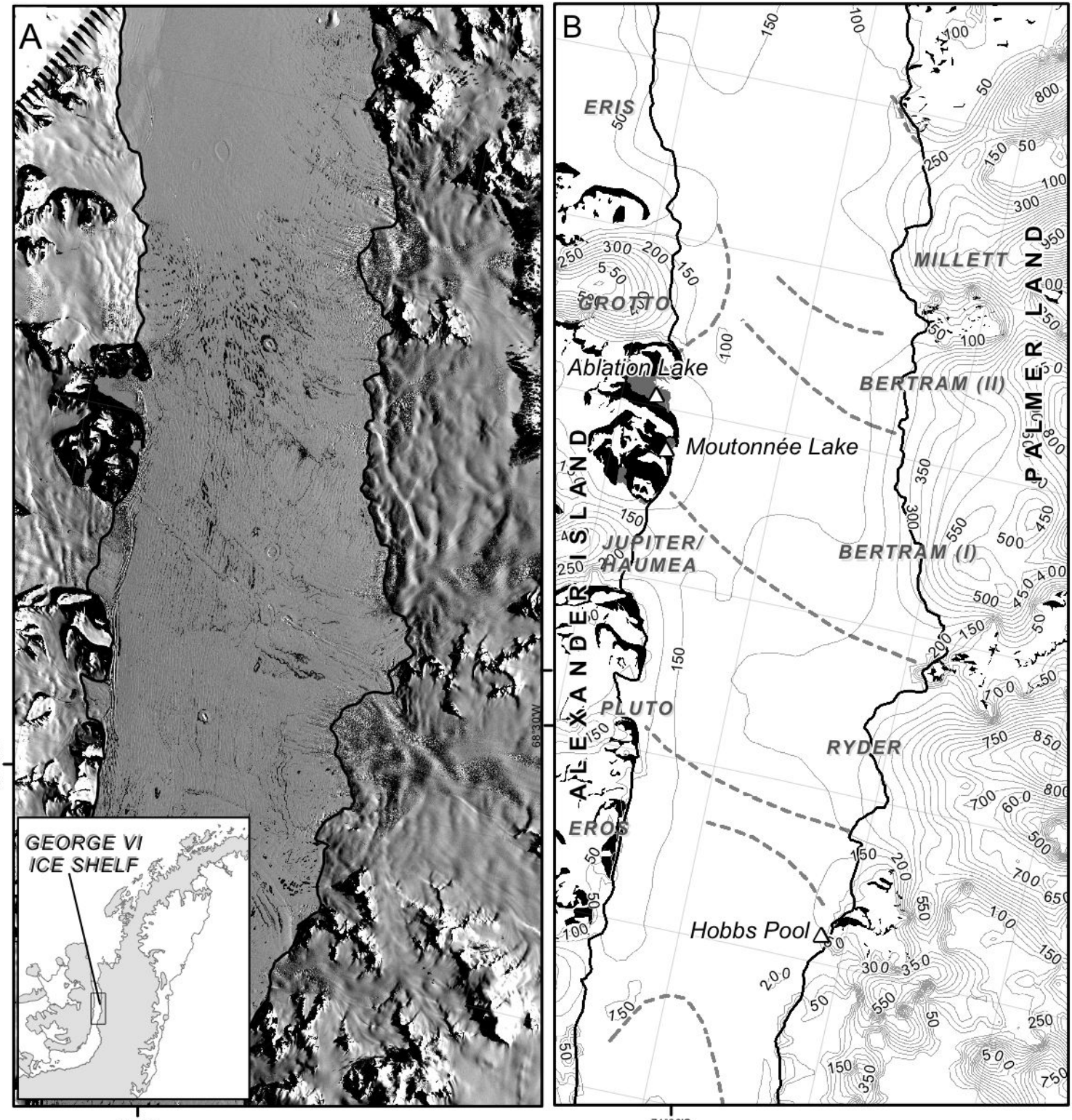
A
B
GEORGE VI
ICE SHELF
ERIS
GROTTO
MILLETT
Ablation Lake
BERTRAM (II)
Moutonnée Lake
ALEXANDER ISLAND
JUPITER/
HAUMEA
BERTRAM (I)
PALMER LAND
PLUTO
RYDER
EROS
Hobbs Pool
68°30'W
71°30'S

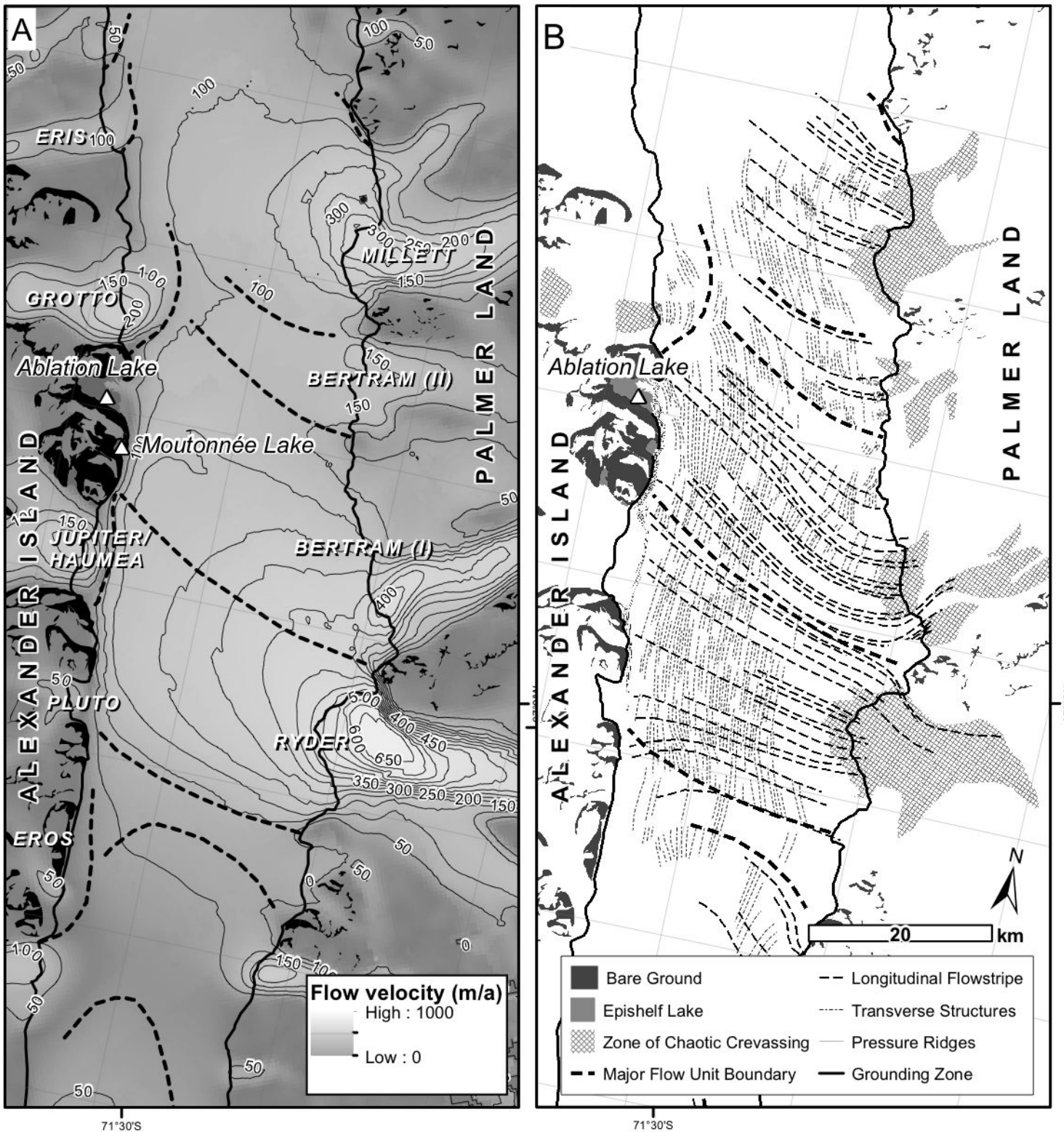
A
B
ERIS
MILLETT
GROTTO
Ablation Lake
Moutonnée Lake
BERTRAM (II)
BERTRAM (I)
JUPITER/
HAUMEA
PLUTO
RYDER
EROS
ALEXANDER ISLAND
PALMER LAND
Flow velocity (m/a)
High : 1000
Low : 0
N
20
km
Bare Ground
Epishelf Lake
Zone of Chaotic Crevassing
Major Flow Unit Boundary
Longitudinal Flowstripe
Transverse Structures
Pressure Ridges
Grounding Zone
71°30'S
67°0'W

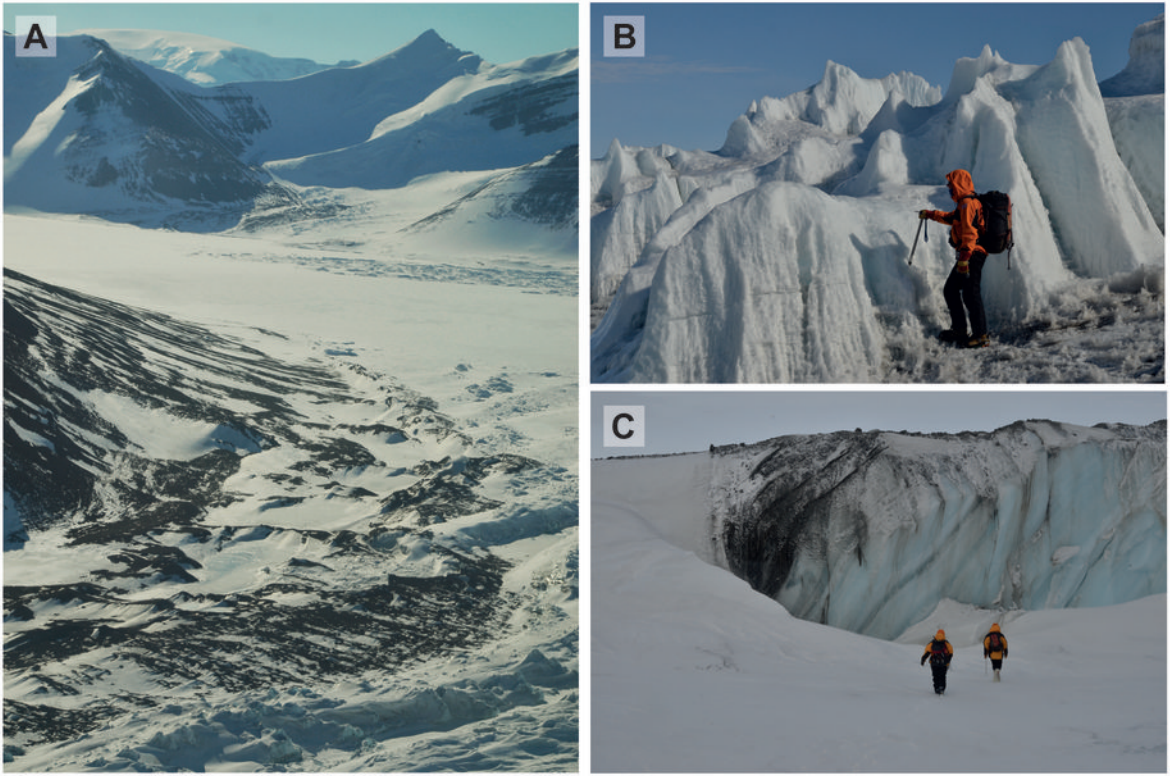
A
B
C

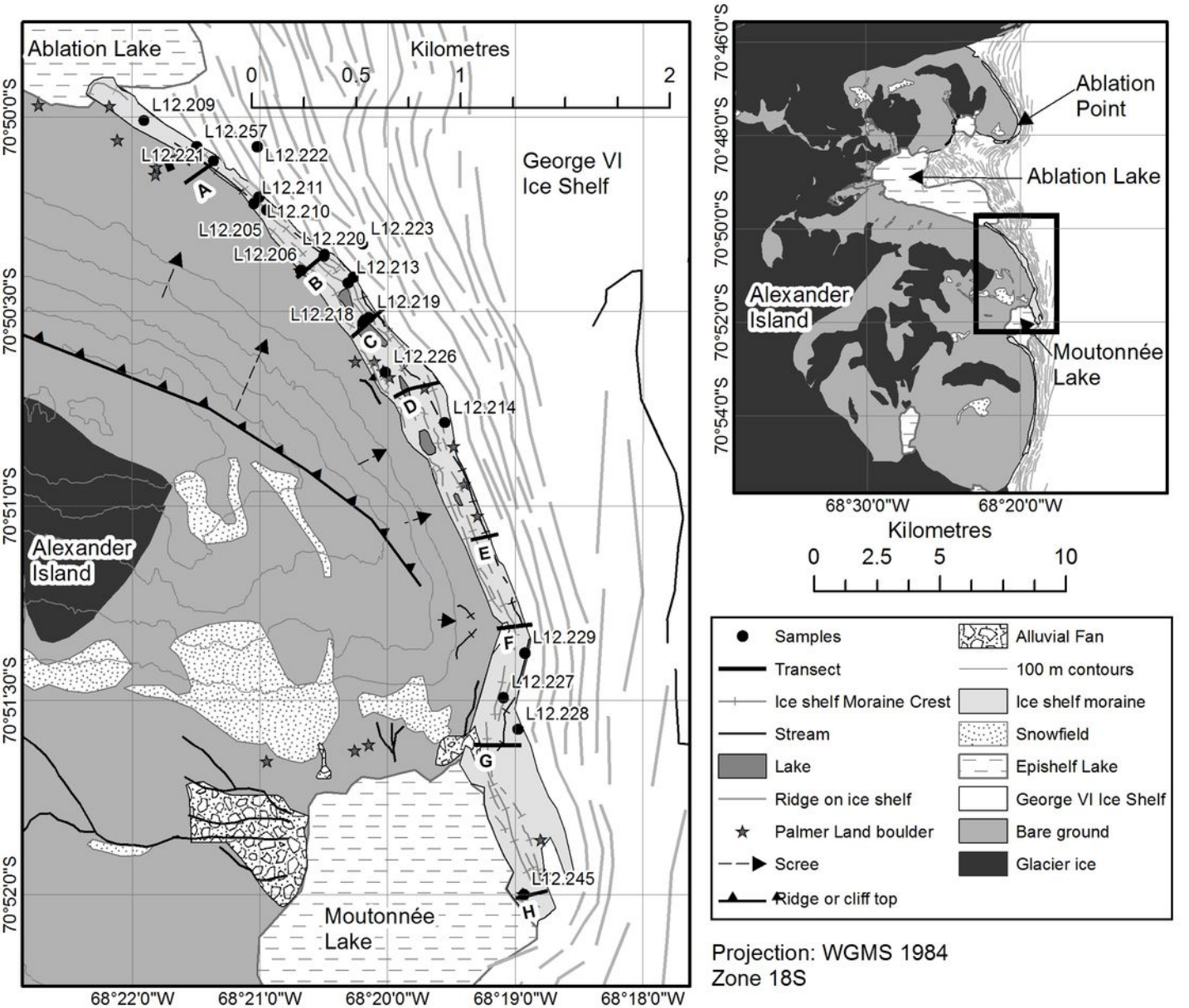
Ablation Lake
Kilometres
0
0.5
1
2
L12.209
L12.257
L12.221
L12.222
L12.211
L12.210
L12.205
L12.220
L12.223
L12.206
L12.213
L12.219
L12.218
L12.226
L12.214
L12.229
L12.227
L12.228
L12.245
A
B
C
D
E
F
G
H
George VI
Ice Shelf
Alexander
Island
Moutonnée
Lake
70°50'0"S
70°50'30"S
70°51'0"S
70°51'30"S
70°52'0"S
68°22'0"W
68°21'0"W
68°20'0"W
68°19'0"W
68°18'0"W
70°46'0"S
70°48'0"S
70°50'0"S
70°52'0"S
70°54'0"S
Ablation
Point
Ablation Lake
Alexander
Island
Moutonnée
Lake
68°30'0"W
68°20'0"W
Kilometres
0
2.5
5
10
Samples
Transect
Ice shelf Moraine Crest
Stream
Lake
Ridge on ice shelf
Palmer Land boulder
Scree
Ridge or cliff top
Alluvial Fan
100 m contours
Ice shelf moraine
Snowfield
Epishelf Lake
George VI Ice Shelf
Bare ground
Glacier ice
Projection: WGMS 1984
Zone 18S

0
50
100
150
200
250
metres (no vertical exageration)
metres
20
10
0
A
terrace
old degrded moraines
ice-cored moraine
ice shelf
stone stripes
polygons and snow patches
snow
debris flows
crack
A'
70.83618°S
68.35988°W
70.83532°S
68.35435°W
B
ice-cored moraine
ice shelf
terrace
stone stripes
contraction cracks
moss
boulder cluster
snow
ice
B'
70.84023°S
68.34527°W
granite boulder (cosmo)
70.83925°S
68.34158°W
C
ice-cored moraine
ice shelf
debris flows
pond
ice cliff
C'
scree
colluvium
colluvium/snow
snow on frozen lake
70.842783°S
68.33807°W
70.25822°S
68.33383°W
D
old degraded moraines
ice-cored moraine
terrace
scree
4 shorelines
crevasse 30cm
collapsed face
debris-flows ponds
ice cliff
pond (muddy)
D'
snow on pond
lake
70.84540°S
68.33266°W
70.84490°S
68.32925°W
E
ice-cored moraines
ice shelf
scree
collapsing face/gypsum
ponds
debris-flows
snow
pond
snow
E'
70.85153°S
68.32252°W
70.85125°S
68.31889°W
F
old degraded moraine and bedrock
ice-cored moraines
ice shelf
scree
pebble lag
cobble lag
bedrock
6m gneiss boulder
snow
debris-flows
F'
70.85528°S
68.31905°W
70.85509°S
68.31445°W
G
old degraded moraine
ice-cored moraines
Moutonnée Lake
split boulder
contraction cracks
debris flows
kettles
stream-sorting
drained lake "mushrooms"
G'
70.86026°S
68.32209°W
70.86028°S
68.31580°W
H
Moutonnée Lake
weathered basalt bedrock
patchy basalt bedrock
snow
snow bank
pond
ice-cliff
ice-pressure
burried ridge
H'
70.86685°S
68.31669°W
70.86654°S
68.31256°W
0
50
100
150
200
250
metres (no vertical exageration)
Lithofacies
angular boulders-scree
sandy gravel
muddy gravel
diamicton (clast-rich muddy)
sand
cobble/boulder lag on surface
bedrock; volcanic (Jurassic-Cretaceous)
Ice shelf
glacier ice with near-vertical foliation
tide - cracks
ice pinnacles
ice mushrooms on debris-covered ice

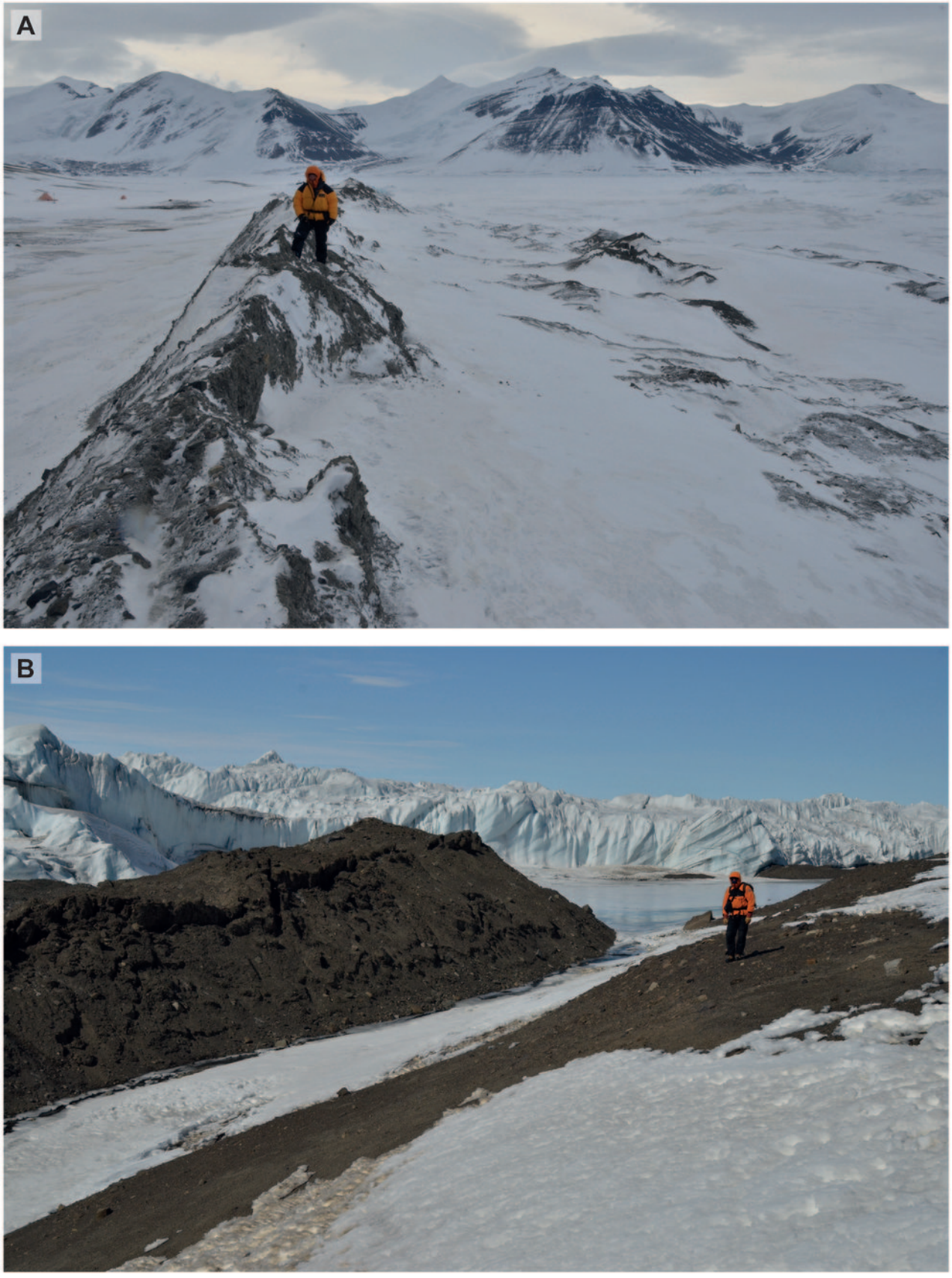
A
B

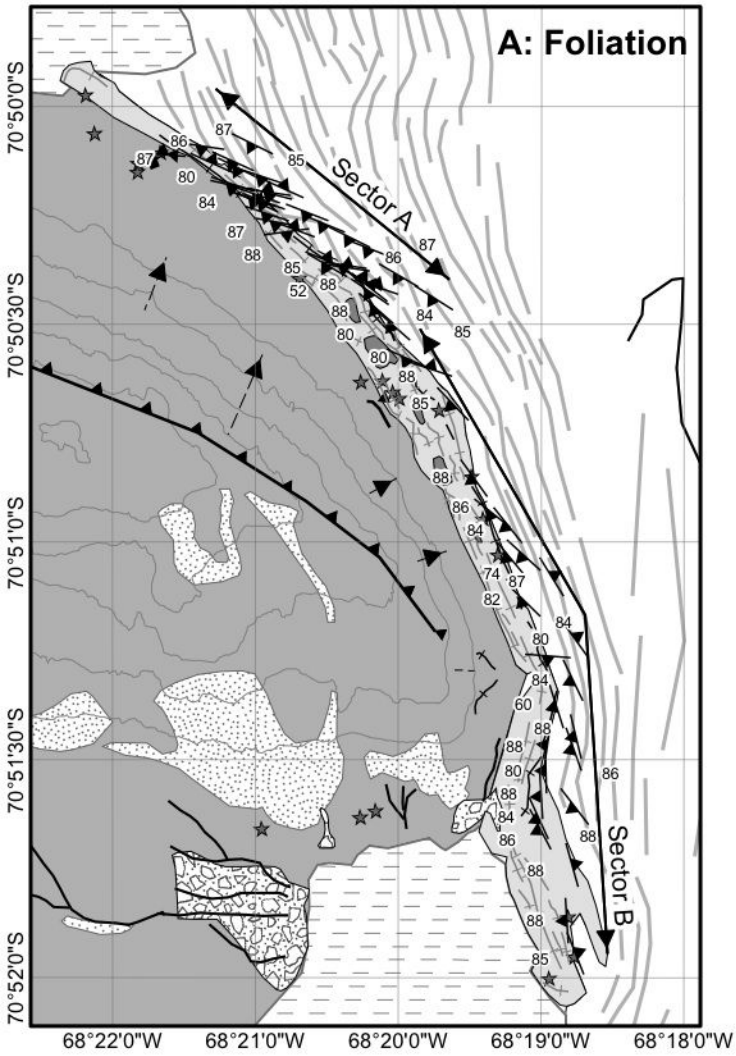

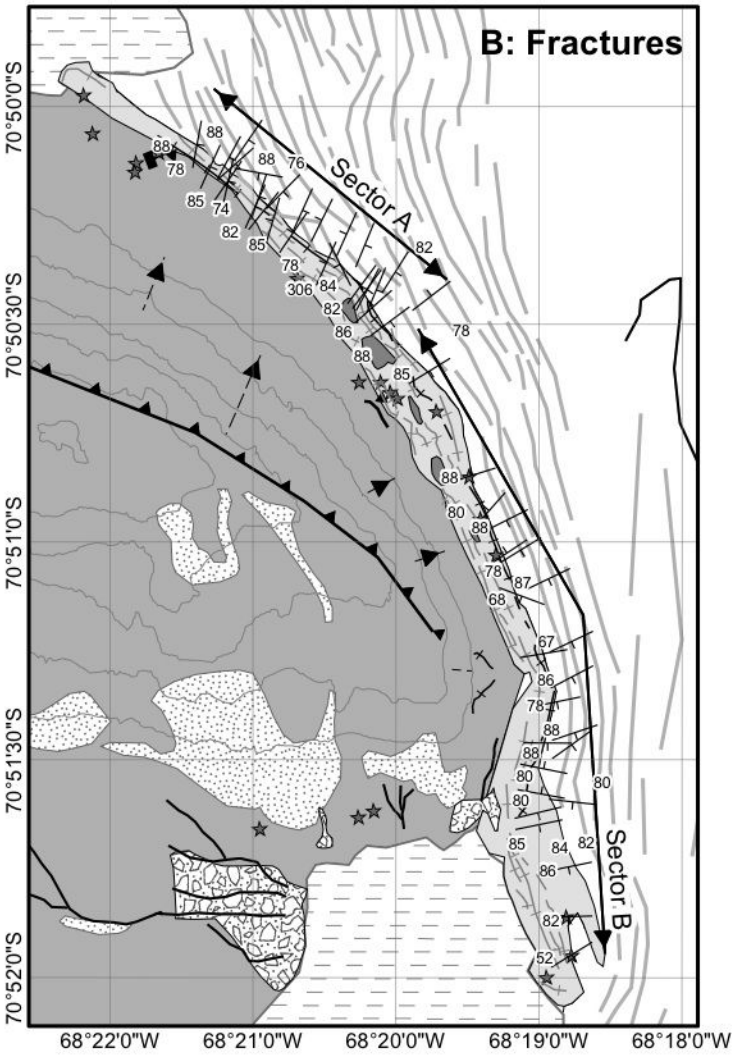

Foliation, Section A
n=59

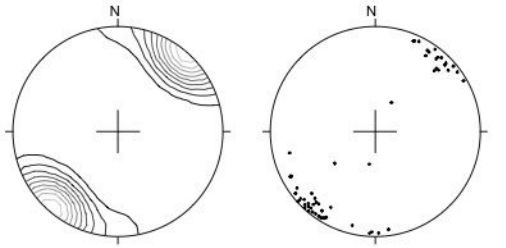

$S_1 = 0.8998$
$S_2 = 0.0639$
$S_3 = 0.0364$
$V_1 = 218.20^{o}$

Fractures, Section A
n=53

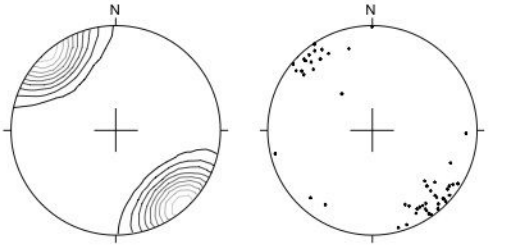

$S_1 = 0.8759$
$S_2 = 0.0977$
$S_3 = 0.0263$
$V_1 = 139.40^{o}$

Foliation, Section B
n=34

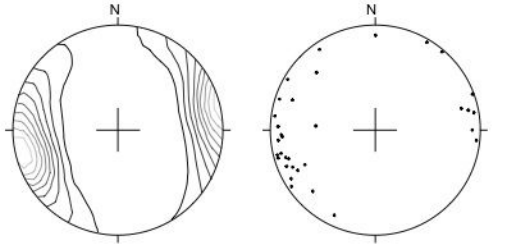

$S_1 = 0.7975$
$S_2 = 0.1878$
$S_3 = 0.0147$
$V_1 = 258.60^{o}$

Fractures, Section B
n=35

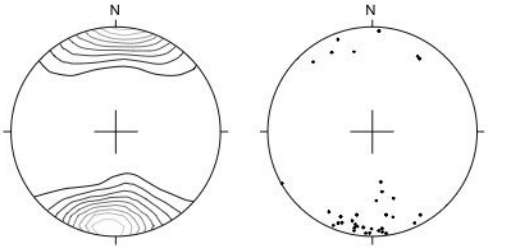

$S_1 = 0.8652$
$S_2 = 0.1036$
$S_3 = 0.0312$
$V_1 = 181.40^{o}$

Base camp
Samples
Transect
Foliation
Fractures
Ice shelf Moraine Crest
Stream

Ice shelf ridge
Lake
Stream
Palmer Land boulder
Scree
Ridge or cliff top
Alluvial Fan
100 m contours

Moraine ridge crest
Ice shelf moraine
Snowfield
Epishelf Lake
Epishelf Lake
George VI Ice Shelf
Bare ground

Kilometres
0 0.5 1 2

N

Projection: WGMS 1984
Zone 21S

Lithofacies/abundance		Description	Samples	Interpretation
Clast-rich sandy diamicton ****		Massive and poorly sorted, with up to 50% gravel clasts. Mixed local and exotic lithologies up to boulder-size; predominantly SA, SR. 6-20% striated and 8-16% faceted clasts.	*L12.207* **L12.209** *L12.212* *L12.213* **L12.214** **L12.218** *L12.221* *L12.224* *L12.226* *L12.229*	Derived from near-vertical foliation incorporating basal debris; melting out *in situ*. Local (mainly) Palmer Land clasts both represented.
Sandy gravel (muddy) *****		Massive to weakly stratified, poorly sorted, with >50% clasts. Predominantly local clasts up to boulder size and roundness typically SA, A. 2-12% striated and 4-12% faceted clasts.	*L12.205* **L12.206** *L12.208* *L12.210L 12.211* **L12.219** *L12.220* *L12.228*	Derived from near-vertical foliation incorporating local subglacial bedrock; melting out *in situ*.
Sandy gravel **		Massive to weakly stratified cobbles-granules in sandy matrix, moderately well sorted. Mixed local and exotic clasts up to pebble/cobble-size; predominantly SR, R		Derived from foliated ice, but reworked by debris-flows and small streams within moraine.
Sand *		Patches of medium to coarse well-sorted sand on ice-shelf surface; in stream-beds and ponds.	**L12.223**	Aeolian debris accumulated on ice-shelf surface and concentrated by flowing water in late summer.

Figure 8. Principal lithofacies associated with ice-shelf moraine and adjacent foliated glacier ice. Relative abundance indicated from * (least) to ***** (most). Clast roundness: R = rounded, SR = subrounded; SA = subangular; A = angular. Sample numbers in bold refer to representative sedimentological data in Figure 9; numbers in italics represent the full data-set in *Supplementary Material,* Figure S4. Sample locations are illustrated in Figure 4.

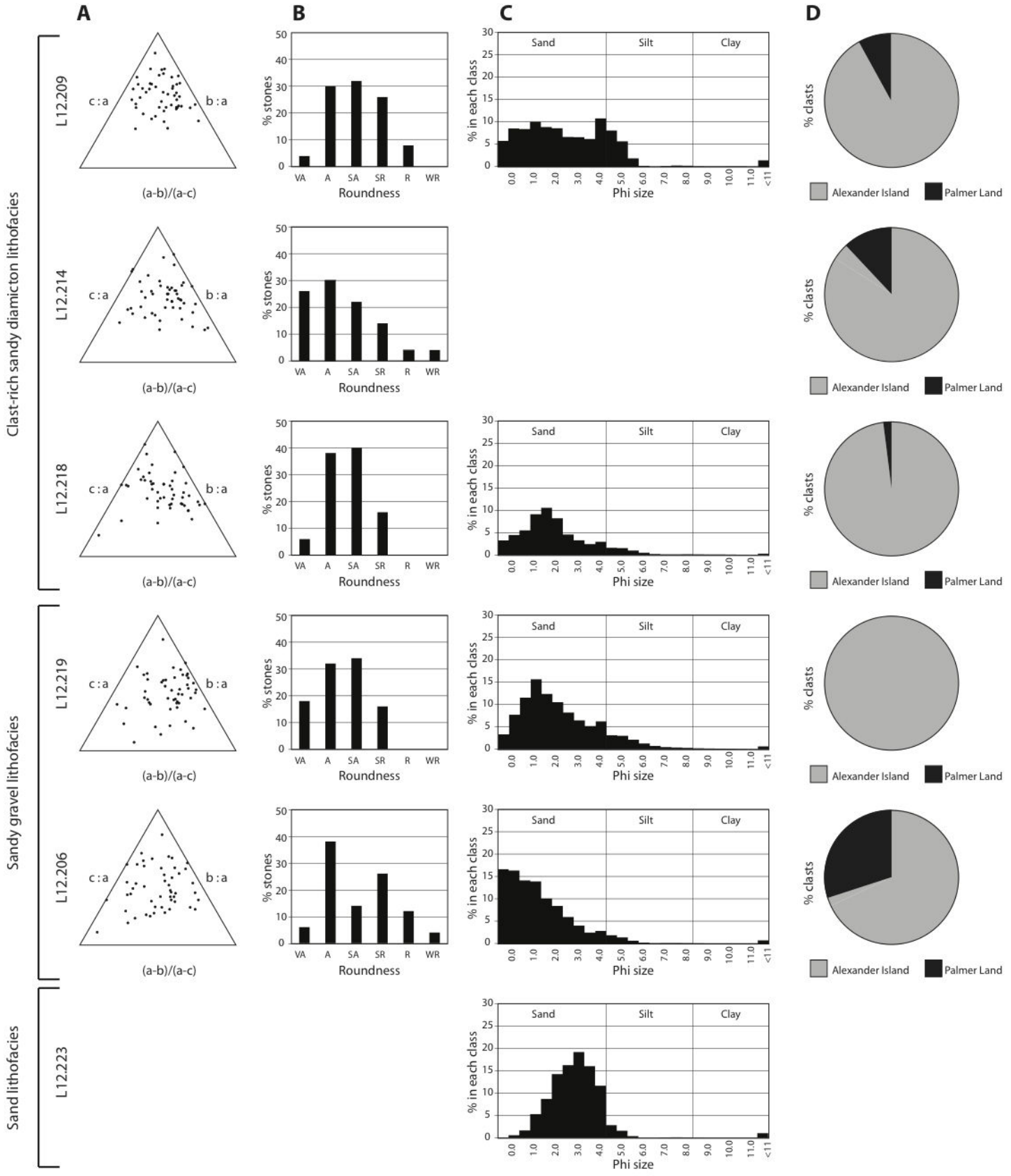
A
B
C
D
Clast-rich sandy diamicton lithofacies
Sandy gravel lithofacies
Sand lithofacies
L12.209
L12.214
L12.218
L12.219
L12.206
L12.223
c:a
b:a
(a-b)/(a-c)
% stones
VA A SA SR R WR
Roundness
% in each class
Sand
Silt
Clay
Phi size
% clasts
Alexander Island
Palmer Land

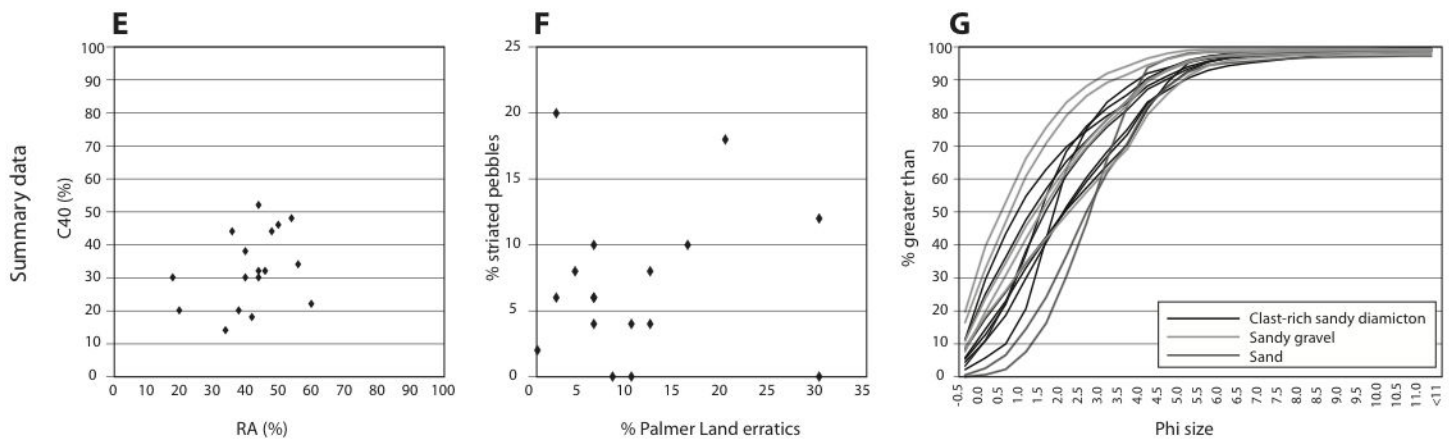
Summary data
E
C40 (%)
RA (%)
F
% striated pebbles
% Palmer Land erratics
G
% greater than
Phi size
Clast-rich sandy diamicton
Sandy gravel
Sand

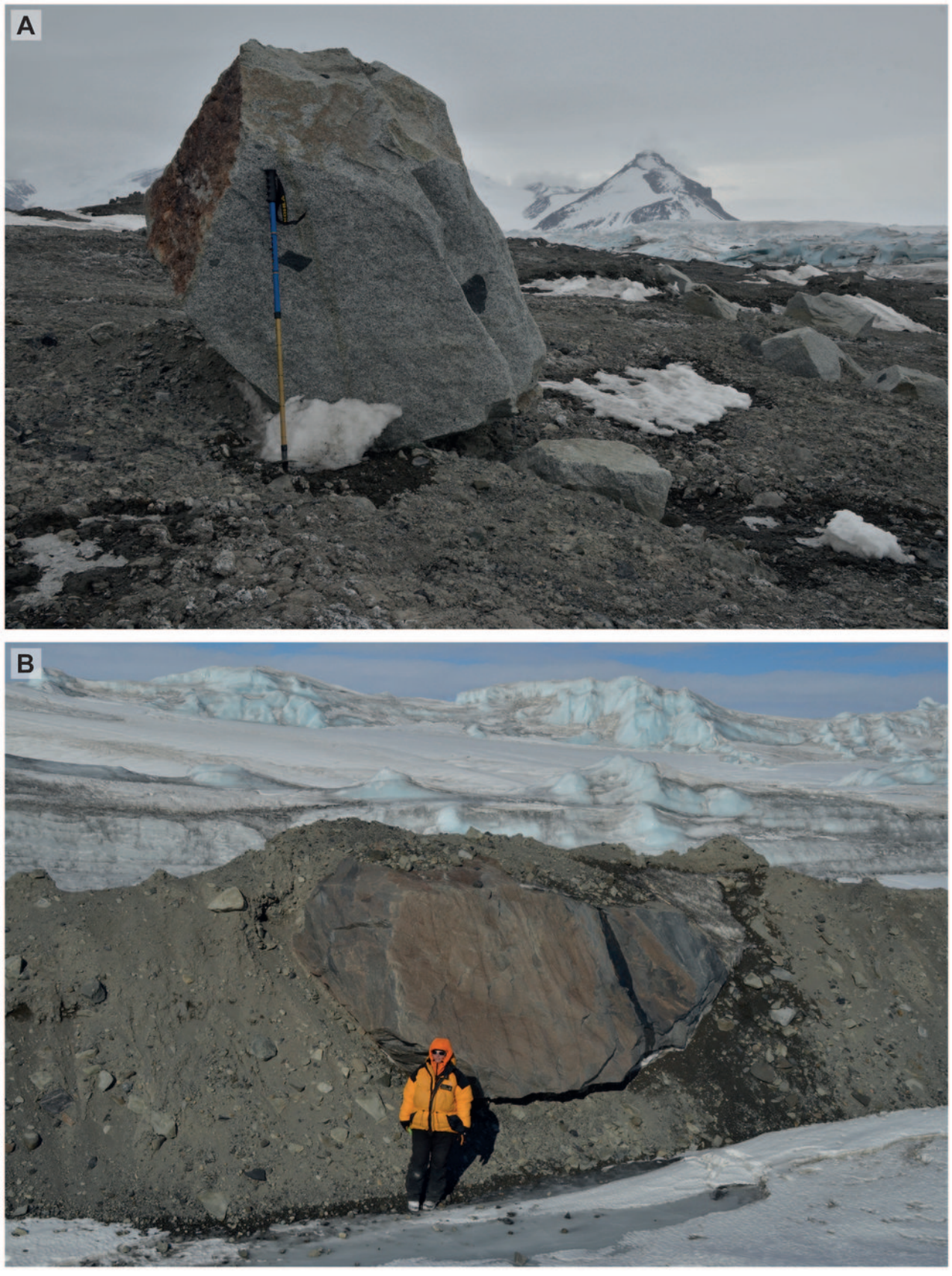
A
B

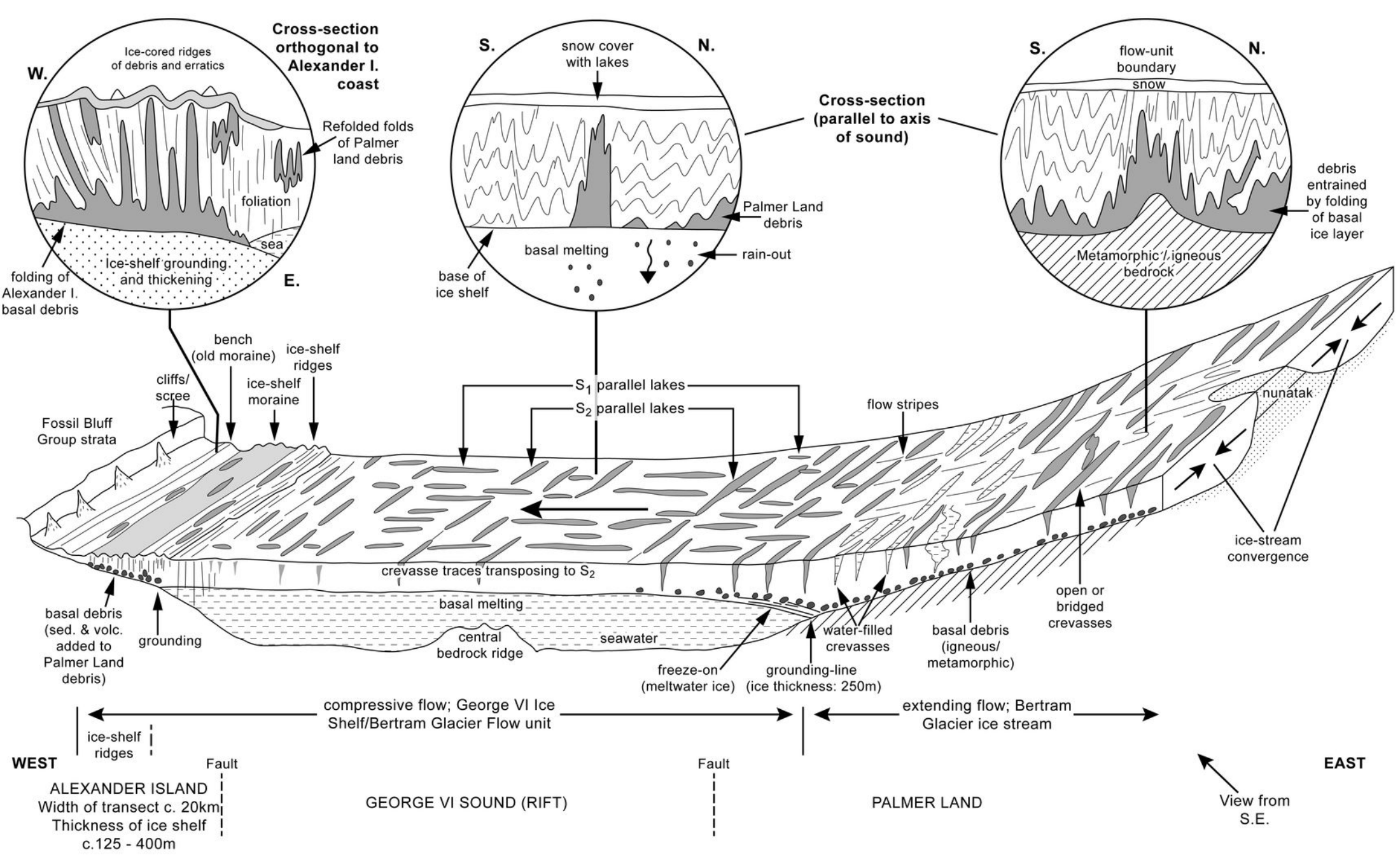
Cross-section orthogonal to Alexander I. coast
W.
E.
Ice-cored ridges of debris and erratics
Refolded folds of Palmer land debris
foliation
sea
Ice-shelf grounding and thickening
folding of Alexander I. basal debris
S.
N.
snow cover with lakes
Palmer Land debris
basal melting
rain-out
base of ice shelf
Cross-section (parallel to axis of sound)
S.
N.
flow-unit boundary
snow
debris entrained by folding of basal ice layer
Metamorphic / igneous bedrock
bench (old moraine)
ice-shelf ridges
cliffs/ scree
ice-shelf moraine
Fossil Bluff Group strata
S1 parallel lakes
S2 parallel lakes
flow stripes
nunatak
ice-stream convergence
crevasse traces transposing to S2
basal melting
central bedrock ridge
seawater
basal debris (sed. & volc. added to Palmer Land debris)
grounding
freeze-on (meltwater ice)
grounding-line (ice thickness: 250m)
water-filled crevasses
basal debris (igneous/ metamorphic)
open or bridged crevasses
compressive flow; George VI Ice Shelf/Bertram Glacier Flow unit
extending flow; Bertram Glacier ice stream
ice-shelf ridges
WEST
EAST
Fault
Fault
ALEXANDER ISLAND
Width of transect c. 20km
Thickness of ice shelf c.125 - 400m
GEORGE VI SOUND (RIFT)
PALMER LAND
View from S.E.